


# Transcription factors *Bcl11a* and *Bcl11b* are required for the production and differentiation of cortical projection neurons

Heng Du<sup>1</sup>, Ziwu Wang<sup>1</sup>, Rongliang Guo<sup>1</sup>, Lin Yang<sup>1</sup>, Guoping Liu<sup>1</sup>, Zhuangzhi Zhang<sup>1</sup>, Zhejun Xu<sup>1</sup>, Yu Tian<sup>1</sup>, Zhengang Yang<sup>1</sup> , Xiaosu Li<sup>1</sup>, Bin Chen<sup>2</sup>

<sup>1</sup>State Key Laboratory of Medical Neurobiology and MOE Frontiers Center for Brain Science, Institute of Pediatrics, Children's Hospital of Fudan University, Institutes of Brain Science, Fudan University, Shanghai 200032, China,

<sup>2</sup>Department of Molecular, Cell and Developmental Biology, University of California, Santa Cruz, CA 95064, USA

\*Address correspondence to Xiaosu Li, State Key Laboratory of Medical Neurobiology and MOE Frontiers Center for Brain Science, Institute of Pediatrics, Children's Hospital of Fudan University, Institutes of Brain Science, Fudan University, 138 Yixueyuan Road, Shanghai 200032, China. Email: [lixiaosu@fudan.edu.cn](mailto:lixiaosu@fudan.edu.cn); Bin Chen, Department of Molecular, Cell and Developmental Biology, University of California, 1156 High Street, Santa Cruz, CA 95064, USA. Email: [bchen@ucsc.edu](mailto:bchen@ucsc.edu)

The generation and differentiation of cortical projection neurons are extensively regulated by interactive programs of transcriptional factors. Here, we report the cooperative functions of transcription factors *Bcl11a* and *Bcl11b* in regulating the development of cortical projection neurons. Among the cells derived from the cortical neural stem cells, *Bcl11a* is expressed in the progenitors and the projection neurons, while *Bcl11b* expression is restricted to the projection neurons. Using conditional knockout mice, we show that deficiency of *Bcl11a* leads to reduced proliferation and precocious differentiation of cortical progenitor cells, which is exacerbated when *Bcl11b* is simultaneously deleted. Besides defective neuronal production, the differentiation of cortical projection neurons is blocked in the absence of both *Bcl11a* and *Bcl11b*: Expression of both pan-cortical and subtype-specific genes is reduced or absent; axonal projections to the thalamus, hindbrain, spinal cord, and contralateral cortical hemisphere are reduced or absent. Furthermore, neurogenesis-to-gliogenesis switch is accelerated in the *Bcl11a*-CKO and *Bcl11a/b*-DCKO mice. *Bcl11a* likely regulates neurogenesis through repressing the *Nr2f1* expression. These results demonstrate that *Bcl11a* and *Bcl11b* jointly play critical roles in the generation and differentiation of cortical projection neurons and in controlling the timing of neurogenesis-to-gliogenesis switch.

**Key words:** *Bcl11a*; *Bcl11b*; cortical projection neurons; neurogenesis; *Nr2f1*.

## Introduction

Cortical projection neurons, or pyramidal neurons, constitute approximately 70–80% of the neuronal population in the mammalian neocortex, the precise development of which is quintessential for sensory information integration, motor coordination, and cognition (McConnell 1989; Molyneaux et al. 2007; Greig et al. 2013). Cortical neurogenesis begins with the proliferation of neuroepithelial cells which produce cortical radial glial cells (RGCs) located in the ventricular zone (VZ). RGCs divide symmetrically to expand the progenitor pool, or asymmetrically to produce cortical projection neurons (direct neurogenesis) or intermediate progenitor cells (IPCs) that migrate to the subventricular zone (SVZ), where they divide to generate cortical projection neurons (indirect neurogenesis). The projection neurons sequentially populate the cortical layers in an inside-first, outside-last sequences (McConnell 1989, 1995; Leone et al. 2008; Juric-Sekhar and Hevner 2019). As the projection neurons are generated, their subtype identities are established by transcriptional repressors that act in the postmitotic neurons to repress alternate subtype identities

(Alcamo et al. 2008; Chen et al. 2008; McKenna et al. 2011, 2015; Tsyporin et al. 2021). At the end of cortical neurogenesis, cortical RGCs switch from generating excitatory projection neurons to producing inhibitory olfactory bulb interneurons and cortical glia, in a process controlled by *Shh* signaling (Zhang, Liu, et al. 2020; Li et al. 2021).

Recent single-cell RNA-seq analyses (scRNA-seq) have segregated cortical projection neurons into many clusters based on gene expression of individual cells (Tasic et al. 2018). However, cortical projection neurons can also be classified into three broad classes based on axonal projections. The subcerebral neurons that extend their axons into the midbrain, the pons, the medulla oblongata and the spinal cord are located in the layer V. The corticothalamic neurons project their axons into the thalamus. They are located in layer VI. Corticocortical projection neurons extend their axons to other cortical areas either in the ipsilateral (associative projection neurons) or contralateral (commissural projection neurons) hemispheres, and they are distributed across layers II–VI (Molyneaux et al. 2007; Leone et al. 2008; Greig et al. 2013).

A few transcription factors have been identified that are essential for subtype specification and differentiation of cortical projection neurons. For example, *Sox5* regulates the migration and identities of corticofugal projection neurons residing in deep cortical layers, and it does so by directly repressing *Fezf2* expression (Kwan et al. 2008; Lai et al. 2008; Shim et al. 2012). *Tbr1* promotes layer VI corticothalamic neuron subtype identity and represses layer V subcerebral neuronal fate by directly repressing *Fezf2* and restricting corticospinal tract outgrowth (Hevner et al. 2001; Bedogni et al. 2010; Han et al. 2011; McKenna et al. 2011). *Fezf2* is expressed in both layer V subcerebral neurons and in layer VI corticothalamic neurons and regulates the identities of both subtypes. It promotes the subtype specification of layer V subcerebral neurons and regulates their axon targeting in part by inhibiting *Tbr1* and *Satb2* expression, the high-level expression of which leads to corticothalamic and corticocortical neuron identities, respectively (Chen et al. 2005, 2008; Molyneaux et al. 2005; Eckler et al. 2014). Recently, it has been shown that in layer VI corticothalamic neurons, *Fezf2* recruits a transcriptional corepressor, *Tle4*, to repress the expression of genes associated with layer V subcerebral neuron features (Tsyporin et al. 2021). The DNA-binding protein that is involved in chromatin remodeling, *Satb2*, is required for the subtype specification and differentiation of multiple cortical projection neuron subtypes. In the callosal neurons, *Satb2* represses the high-level expression of genes associated with subcerebral neuron identity such as *Bcl11b* (Alcamo et al. 2008; Britanova et al. 2008). In the layer V subcerebral neurons, *Satb2* is required for *Fezf2* expression in these neurons, and the mutual regulations between *Satb2* and *Fezf2* ensure that the subcerebral neuron identity is established, as evidenced by the facts layer V subcerebral neurons and axons are missing in mice deficient in either gene (Chen et al. 2008; McKenna et al. 2015).

Zinc-finger transcription factor family Bcl11 proteins (*Bcl11a* and *Bcl11b*) share 55% identity at amino acid level. They were first identified by their functions in the immune and hematopoietic systems (Lessel et al. 2018; Liu et al. 2018; Simon et al. 2020). In the central nervous system, they are mainly expressed in the cerebral cortex, olfactory bulb, striatum, and dorsal spinal cord (Leid et al. 2004). *BCL11A* (also known as *CTIP1*) has been implicated in neocortical dysplasia, autism spectrum disorders, neuropsychiatric disorders linked with intellectual deficiency, epileptic encephalopathy, dyspraxia, and hypotonia in human patients (Sanders et al. 2015; Soblet et al. 2018; Yoshida et al. 2018). *BCL11B* (also known as *CTIP2*) has been linked to a number of neurodegenerative disorders including Alzheimer's disease, Huntington's disease, schizophrenia, and amyotrophic lateral sclerosis (Lennon et al. 2016, 2017).

Recent studies have reported that *Bcl11a* and *Bcl11b* are expressed in nonoverlapping populations of neurons in the murine cerebral cortex and have distinct functions (Arlotta et al. 2005; Wiegrefe et al. 2015;

Greig et al. 2016; Woodworth et al. 2016). *Bcl11b* is expressed in layer V subcerebral neurons and is essential for the fasciculation, refinement, and elaboration of the axonal projections to the spinal cord (Arlotta et al. 2005). *Bcl11a* is expressed in projection neurons in all cortical layers. Within the deep cortical layers, it is not expressed in the *Bcl11b*<sup>+</sup> layer V subcerebral neurons (Woodworth et al. 2016). *Bcl11a* is critical for the migration of upper layer projection neurons by repressing the expression of *Sema3c* and regulates the morphology of these neurons in a mechanism independent of *Sema3c* (Wiegrefe et al. 2015). In the deep cortical layers, *Bcl11a* promotes the acquisition of corticothalamic and callosal subtype identities and represses the layer V subcerebral identity (Wiegrefe et al. 2015; Woodworth et al. 2016). In addition, *Bcl11a* regulates cortical arealization by driving sensory-specific differentiation, including gene expression, output connectivity, and formation of topographic maps (Greig et al. 2016). Taken together, these studies indicate that these two related transcriptional factors control distinct development processes of cortical projection neurons, but whether they have joint functions in cortical neurogenesis and projection neuron differentiation remains to be addressed.

Here, we show that *Bcl11a* is expressed in RGCs and intermediate progenitors, and it regulates the proliferation and differentiation of cortical progenitor cells, as well as the timing of neurogenesis and gliogenesis switch. We show that *Bcl11a* binds to and likely directly represses the transcription of *Nr2f1*, a transcription factor previously shown to inhibit the proliferation and promote the differentiation of cortical progenitor cells (Faedo et al. 2008). We discover that beyond their own unique and seemingly antagonizing functions in specifying corticothalamic and deep-layer callosal versus layer V subcerebral neuronal subtype identities, *Bcl11a* and *Bcl11b* redundantly promote cortical projection neuron subtype specification and differentiation: In the *Bcl11a* and *Bcl11b* double mutant mice, expression of cortical projection neuronal genes, especially of the corticothalamic and layer V subcerebral neuronal genes, is severely reduced or almost absent; and consistent with these cellular and molecular defects, the corticothalamic axons are completely missing in the thalamus and the subcerebral axons fail to reach the pyramidal decussation.

## Materials and Methods

### Mice

*Bcl11a*<sup>Flox/Flox</sup> (Liu et al. 2003; Yu et al. 2012), *Bcl11b*<sup>Flox/Flox</sup> (Li et al. 2010), *Emx1-cre*<sup>+/-</sup> (Gorski et al. 2002), and *IS*<sup>Flox/Flox</sup> (He et al. 2016; Li et al. 2021) mice were previously described. These mice were maintained in a mixed genetic background of C57BL/6J and CD1. The date of vaginal plug detection was designated as embryonic day 0.5 (E0.5) and the day of birth was designated as postnatal day 0 (P0). All animal experiments described in this

study were approved in accordance with institutional guidelines at Fudan University Shanghai Medical College.

### 5-Bromo-2'-deoxyuridine/5-Ethynyl-2'-deoxyuridine Labeling

For cell cycle length analysis, timed pregnant females were intraperitoneally injected with 5-bromo-2'-deoxyuridine (BrdU) (50 mg/kg in 0.9% NaCl) at E13.5 or E15.5; 5-ethynyl-2'-deoxyuridine (EdU) (10 mg/kg in DMSO) was intraperitoneally injected 1.5 h after BrdU injection. Embryonic brains were collected 30 min after EdU injection, followed by immersion fixed for 8 h in 4% PFA, cryoprotected in 30% sucrose for at least 24 h, frozen in the embedding medium, and sectioned at 12  $\mu$ m using a cryostat. EdU was detected using the Click-iT EdU Cell Proliferation Kit (ThermoFisher, USA), following the manufacturer's instruction (Zhang et al. 2020). Briefly, the sections on slides were fixed in 4% PFA for 15 min, followed by washing in 1 $\times$  phosphate buffered saline (PBS) twice and permeabilization with 0.5% Triton X-100 for 20 min at room temperature. Reaction cocktail was prepared freshly according to manufacturer's instruction. The permeabilization buffer was replaced with reaction cocktail and the slides were incubated for 30 min at room temperature, protected from light. We removed the reaction cocktail, washed with 1 $\times$  PBS, performed the BrdU immunocytochemistry, and proceeded to imaging and analysis.

For analysis of production of deep-layer projection neurons, female mice were given single intraperitoneal injections of BrdU at E13.5. Brains were collected at P0 and processed for BrdU immunocytochemistry.

### Tissue Preparation

Postnatal mice were perfused transcardially with 1 $\times$  PBS (pH 7.4), followed by 4% paraformaldehyde (PFA) in 1 $\times$  PBS. Postnatal brains were dissected and postfixed overnight in 4% PFA; embryonic brains were immersion fixed for at least 12 h in 4% PFA, cryoprotected in 30% sucrose for at least 24 h, frozen in the embedding medium, and cryosectioned at 8, 12, or 20  $\mu$ m using a cryostat (CM1950, Leica, USA).

### Histology

The sections on slides were fixed in 4% PFA for at least 10 min, washed in double distilled water twice, followed by staining in a cresyl violet solution (Beyotime, C0117) for 1–5 min at room temperature. After cleared in distilled water, the slides were serially dehydrated in 70%, 80%, and 95% and two passes in 100% ethanol (3 min for each step). All slides were then given two 5-min passes in 100% dimethylbenzene and coverslips were applied with neutral balsam (Wang et al. 2018).

### Immunohistochemistry

For BrdU detection, 8- or 12- $\mu$ m-thick coronal sections were treated with 2 N HCl at room temperature for an hour, neutralized in 0.1 M borate buffer (pH 8.6) for

10 min twice, and washed in 1 $\times$  PBS twice. The sections were incubated overnight at 4°C with a rat anti-BrdU antibody (1:200, Accurate Chemical, OBT0030s) (Li et al. 2018).

For Bcl11a, Bcl11b, Pax6, Eomes, Tuj1, Aldh111 immunohistochemistry, sections on slides were boiled in 10 mM sodium citrate briefly for antigen retrieval. The sections were permeabilized with 0.05% Triton X-100 for 30 min and incubated in a blocking buffer (5% donkey serum and 0.05% Triton X-100 in 1 $\times$  PBS) for 2 h. The blocking buffer was removed, and the sections were incubated overnight at 4°C with the following primary antibodies diluted in the blocking buffer: rabbit anti-Pax6 (1:2000, MBL, PD022), mouse anti-Pax6 (1:400, BD Pharmingen, 561664), mouse anti-Bcl11a (1:1200, Abcam, ab19487), rat anti-Bcl11b (1:1500, Abcam, ab18465), rabbit anti-Eomes (Tbr2, 1:300, Abcam, ab23345), rat anti-Eomes (Tbr2, 1:500, Thermo Fisher, 12-4875-82), rabbit anti-Dcx (1:2000, Abcam, ab18723), mouse anti-Tuj1 (1:500, Covance, MMS-435P-256), rabbit anti-Tbr1 (1:500, Abcam, ab31940), rabbit anti-PH3 (1:500, Sigma-Aldrich, 06-570), rabbit anti-KI67 (1:500, Vector Labs, VP-K451), mouse anti-NeuN (1:1000, Millipore, MAB-377), rabbit anti-Cleave Caspase-3 (1:500, Cell Signaling, 9616), goat anti-Foxp2 (1:500, Santa Cruz, sc-21069), rabbit anti-Aldh111 (1:1500, Abcam, ab87117), rabbit anti-Gfap (1:2000, Dako, Z0334), goat anti-Egfr (1:500, R&D, AF1280), rabbit anti-Olig2 (1:1000, Millipore, MAB9610), and goat anti-Sox10 (1:300, R&D, AF2864).

The sections were incubated with secondary antibodies against the appropriate species for 90 min at room temperature (all from Jackson, 1:500–1:600). Fluorescently stained sections were then washed, counterstained with 4',6-diamidino-2-phenylindole (DAPI) (Sigma, 200 ng/mL) for 2–5 min, and coverslipped with Gel/Mount (Biomedex, Foster City, CA).

### In Situ RNA Hybridization

All in situ RNA hybridization experiments were performed using digoxigenin riboprobes on 20- $\mu$ m cryostat sections as previously described (Guo et al. 2019; Liu et al. 2019). Riboprobes were made from cDNAs amplified by PCR using the following primers:

*Cnr1* Forward: AGAGCTATGGCATACAGGAGTGGTG  
*Cnr1* Reverse: GACTTGATTATTAGTAGGCGCCAC  
*Plk2* Forward: GAGTAGGGAGAGAGACTGGTGCTCG  
*Plk2* Reverse: ATCTGGAAGTGTGTGGCAACAGCT  
*Rorb* Forward: GCCAATGTTTCAAGATGTGCTAGGA  
*Rorb* Reverse: CTGGGATGTAACCTGCTTGATTGA  
*Satb2* Forward: AGTTCTTGAACCCACCCATTC  
*Satb2* Reverse: GAGCCTTCCTCACTGTCACTTCTCCT  
*Cux1* Forward: CAAGATGAGAGCGAACAGTCCAGA  
*Cux1* Reverse: CTAATTCTAGGCTGGATCGGGTCA  
*Tle4* Forward: CTGTGGCAAATGTTTTGTAAGCA  
*Tle4* Reverse: AGTTGCCCAAATAGACTCAAAGGAA  
*Ppp1r1b* Forward: ATGAGCCCCAGAGAGATGGAACT  
*Ppp1r1b* Reverse: ATTACAGCGTAGGAGGGGTTTCAGG  
*Sox5* Forward: ACATCAAGGAAGAGATCCAGGCTG

Sox5 Reverse: CAAACACAGGCTCTTGTTCCTCT  
 Foxp1 Forward: ACACTCTAGGGACATGGCAGATTCA  
 Foxp1 Reverse: TGGTTCCATTGCCTACATAGTCTGC  
 Nr2f1 Forward: GAAAACAGCAGGAACCACAACAA  
 Nr2f1 Reverse: TGAAGAACAGCCTCGACAACATATA  
 Shhn1 Forward: GAAAACAGGAGAGACGGACAGTTCC  
 Shhn1 Reverse: GCAGTGAAGGGAGAAAAACAATGTG  
 Dync111 Forward: CACTGTCTCTACCGATGGCAAATG  
 Dync111 Reverse: AAGATGCCACGGGATACTGATACA  
 Otx1 Forward: TCAATTTCAACTCTCCCGACTGTC  
 Otx1 Reverse: TGGACGCTAAAACAAGAGAGATGC  
 Nfe2l3 Forward: TGATTTAGGTGCTGTAGGAGGCTG  
 Nfe2l3 Reverse: GGAACATGTGGATTCTCCCAACTT

### Image Acquisition and Analysis

Bright field images (in situ hybridization) and some fluorescent images were imaged with Olympus VS120 slice scanning system using a 4×, 10×, or a 20× objective. Other fluorescent images were taken with Olympus FV1000 confocal microscope system using a 10×, 20×, or a 40× objective. Z-stack confocal images were reconstructed using the FV10-ASW software. All images were merged, cropped, and optimized in Photoshop CC without distortion of the original information.

Analyses were done using GraphPad Prism 7.0 and SPSS Statistics 19.0. Bcl11a expression and its colocalization with Pax6 in the E10.5 (31 250  $\mu\text{m}^2$  area from the VZ) were quantified in three chosen 8- $\mu\text{m}$  sections. PH3<sup>+</sup>, Eomes<sup>+</sup>, Pax6<sup>+</sup>, KI67<sup>+</sup>, and BrdU<sup>+</sup>/EdU<sup>-</sup> cells in the VZ of E15.5 cortices were quantified in three chosen 12  $\mu\text{m}$  sections for each mouse ( $n = 3$  mice). BrdU, NeuN, and Caspase-3 expression in the cortical plates were quantified in three chosen 20- $\mu\text{m}$  sections for each mouse (P0 control, Bcl11a-CKO, Bcl11b-CKO, and Bcl11a/b-DCKO mice were used,  $n = 3$  mice for each genotype). We counted the cell numbers within a 47 610  $\mu\text{m}^2$  area in the cortical plate for each section.

Statistical significance was assessed using unpaired Student's t-test or one-way ANOVA, followed by a Tukey HSD post hoc test. All quantification results were summarized as the mean  $\pm$  standard error of mean (SEM). P-values < 0.05 were considered significant.

### RNA-Seq Analysis

RNA-Seq analyses were performed as previously described (Guo et al. 2019). The E13.5, E15.5 cortical tissue from Bcl11a-CKO, Bcl11a/b-DCKO mice and littermate controls (Bcl11a<sup>Flox/Flox</sup>; Bcl11b<sup>Flox/Flox</sup>), and P0 cortices from Bcl11a-CKO, Bcl11b-CKO, Bcl11a/b-DCKO mice, and littermate controls were dissected ( $n = 3$  mice/genotype/age).

Total RNA was isolated using an RNeasy Mini Kit (QIAGEN) according to the manufacturer's protocol, quantified using NanoDrop ND-2000 and checked for RNA integrity using a bioanalyzer (Agilent Technologies, Santa Clara, CA, USA). RNA-seq libraries were prepared according to the Illumina TruSeq protocol. An average of 15 million reads per sample was obtained. The gene expression level was reported with fragments per kilobase of

exon model per million mapped reads (FPKM) (Trapnell et al. 2012). A gene was considered to be expressed if it had an FPKM > 1. Differentially expressed genes were identified using edgeR. Genes were considered as differentially expressed with a P-value < 0.05. Data from this experiment have been deposited in the GEO database (GSE182990).

### CUT&Tag-Seq Analysis

CUT&Tag assay was performed using dissected E14.5 neocortices of wild-type mice, and a Bcl11a mouse polyclonal antibody as described above, using a previously published protocol (Skene and Henikoff 2017; Skene et al. 2018; Kaya-Okur et al. 2019). Briefly, the single-cell suspensions from brain tissue were prepared by mechanically disruption, followed by digestion for 15 min at 37 °C with 1.4 mg/mL papain,  $3.3 \times 10^{-3}$  mg/mL DNase I in DMEM cell culture medium. Digested tissue were filtered and pelleted at 300 g (RCF) for 5 min at room temperature. Then,  $1 \times 10^5$  cells were washed with 500  $\mu\text{L}$  of wash buffer and centrifuged at 600 g for 3 min at room temperature. Cell pellets were resuspended with 100  $\mu\text{L}$  of wash buffer. Concanavalin A-coated magnetic beads were washed twice with 100  $\mu\text{L}$  binding buffer. Next, 10  $\mu\text{L}$  of activated beads were added and incubated with the cells at room temperature for 10 min. Bead-bound cells were resuspended in 50  $\mu\text{L}$  of antibody buffer. Then, 1  $\mu\text{g}$  of primary antibody (mouse polyclonal anti-Bcl11a antibody) or no antibody (negative control) was added and incubated at room temperature for 2 h. The primary antibody was removed using a magnet stand. A secondary antibody (0.5  $\mu\text{g}$ , goat anti-mouse IgG, Vazyme, Ab206-01) was diluted in 50  $\mu\text{L}$  of Dig-wash buffer and cells were incubated at room temperature for 1 h. Cells were washed three times with Dig-wash buffer to remove unbound antibodies. The Hyperactive pG-Tn5 Transposase (Transposase mix, 4  $\mu\text{M}$ , Vazyme) was diluted 1:100 in 100  $\mu\text{L}$  of Dig-300 buffer. Cells were incubated with 0.04  $\mu\text{M}$  Transposase mix at room temperature for 1 h. Cells were washed three times with Dig-300 buffer to remove unbound Transposase mix. Cells were then resuspended in 300  $\mu\text{L}$  of tagmentation buffer and incubated at 37 °C for 1 h. To terminate tagmentation, 10  $\mu\text{L}$  of 0.5 M EDTA, 3  $\mu\text{L}$  of 10% SDS, and 2.5  $\mu\text{L}$  of 20 mg/mL Proteinase K were added to 300  $\mu\text{L}$  of sample and incubated overnight at 37 °C. DNA was purified using phenol-chloroform-isoamyl alcohol extraction, followed by an ethanol precipitation and RNase A treatment. For library amplification, 24  $\mu\text{L}$  of DNA was mixed with 1  $\mu\text{L}$  of TruePrep Amplify Enzyme (TAE, Vazyme), 10  $\mu\text{L}$  of 5× TruePrep Amplify Enzyme buffer, 5  $\mu\text{L}$  of ddH<sub>2</sub>O, and 5  $\mu\text{L}$  of uniquely barcoded i5 and i7 primers from TruePrep Index Kit V2 for Illumina (Vazyme). A total volume of 50  $\mu\text{L}$  of sample was placed in a Thermocycler using the following program: 72°C for 3 min; 98°C for 30 s; 17 cycles of 98°C for 15 s, 60°C for 30 s, and 72°C for 30 s; 72°C for 5 min and hold at 4°C. To purify the PCR products, 1.2× volumes of VAHTS DNA Clean Beads (Vazyme) were

added and incubated at room temperature for 10 min. Libraries were washed twice with 80% ethanol and eluted in 22  $\mu$ L of ddH<sub>2</sub>O.

Libraries were sequenced on an Illumina NovaSeq platform and 150-bp paired-end reads were generated. All raw sequence data were quality trimmed to a minimum phred score of 20 using trimmomatic. PCR duplicates were removed using Picard MarkDuplicates v1.107. The reads were aligned to the mm10 mouse genome using Bowtie2 version 2.3.4 and subsequently analyzed using MACS2 software version 2.1.4 to detect genomic regions enriched for multiple overlapping DNA fragments (peaks) that we considered to be putative binding sites. Peaks with a false discovery rate lower than 5% were used for further analyses. Visualization of peak distribution along genomic regions of interested genes was performed with IGV.

### scRNA-Seq Dataset Used in this Study

Published scRNA-seq data from 33976 cells from the mid-gestation human neocortex (3 female donors at GW17, GW17, and GW18, and 1 male donor at GW18) (Polioudakis et al. 2019) (the accession number is dbGaP: phs001836) were downloaded from the website [https://www.ncbi.nlm.nih.gov/projects/gap/cgi-bin/study.cgi?study\\_id=phs001836.v1.p1](https://www.ncbi.nlm.nih.gov/projects/gap/cgi-bin/study.cgi?study_id=phs001836.v1.p1). Supplementary Figure S1 in this study was generated using an online interface at <http://geschwindlab.dgsom.ucla.edu/pages/codexviewer>.

The raw gene expression matrix data obtained with Cell Ranger software were processed with standard Seurat workflow. Cells with fewer than 500 detectable genes or with >10% mitochondrial genes were filtered out. A global-scaling normalization method “Log Normalize” was applied. Cell cycle genes were regressed out to mitigate the effects of cell cycle stage. The first 50 PCs were used for clustering. Either TSNE or UMAP was used for dimension-reduction and visualization.

## Results

### Bcl11a Is Expressed in Cortical RGCs and Intermediate Progenitors

Previous studies reported that Bcl11a protein is expressed in the postmitotic projection neurons (Wiegreffe et al. 2015; Greig et al. 2016; Woodworth et al. 2016). We carefully evaluated whether Bcl11a protein is also expressed in cortical RGCs and intermediate progenitors using immunocytochemistry. At E10.5, we found that 93.5% Pax6-expressing (Pax6<sup>+</sup>) cells express Bcl11A, while 92% Bcl11a<sup>+</sup> cells express Pax6 (Fig. 1A–D). At E12.5, Bcl11a protein is expressed in Eomes<sup>+</sup> intermediate progenitors and Dcx<sup>+</sup> immature neurons (Fig. 1E–G). To validate the expression of Bcl11a in cortical RGCs and intermediate progenitors, we performed immunohistochemistry on brain sections from cortex-specific Bcl11a conditional knockout mice (*Emx1-Cre*; *Bcl11a*<sup>Flox/Flox</sup>, or *Bcl11a*-CKO). While Bcl11a protein is detected in the VZ and SVZ

in the control mice, the expression is not detected in the VZ/SVZ of the *Bcl11a*-CKO mice (Fig. 1H,I). Thus, in addition to the cortical projection neurons, Bcl11a protein is expressed in the RGCs, intermediate progenitors, and immature projection neurons during cortical development in mice.

*BCL11A* gene has been implicated in human autism spectrum disorder with impaired neocortical development, and it is a candidate for the 2p15-16.1 microdeletion syndrome, which is associated with intellectual deficiency and neocortical dysplasia (Balci et al. 2015; Sanders et al. 2015; Dias et al. 2016). We examined *BCL11A* expression in fetal brains by analyzing published scRNA-seq data from the mid-gestation human neocortex (GW17-GW18), which provided a high-resolution transcriptome map of 33976 cortical cells (Supplementary Fig. S1A) (Polioudakis et al. 2019). Similar to its expression in mice, *BCL11A* expression is present in human cortical RGCs where the cluster is defined by PAX6, SOX2, and SOX9 expression (Supplementary Fig. S1B–F) and in the EOMES<sup>+</sup> and NEUROG2<sup>+</sup> projection neuron intermediate progenitor cluster (Supplementary Fig. S1B,G,H). In addition, *BCL11A* is widely expressed in human cortical newly generated and mature projection neurons (Supplementary Fig. S1B,I). *BCL11B* is mainly expressed in immature and mature projection neurons (Supplementary Fig. S1C,I). We noted that *BCL11B* is also expressed in some cells in the EOMES<sup>+</sup> intermediate progenitor cluster in the human cortex (Supplementary Fig. S1C,G).

Taken together, our results show that besides its wide expression in cortical projection neurons, Bcl11a is expressed in RGCs and projection neuron intermediate progenitors in the developing mouse and human cortices.

### Premature Neuronal Differentiation of Cortical RGCs in the *Bcl11a*-CKO Mice

To determine the function of Bcl11a in cortical neurogenesis, we generated cortex-specific Bcl11a knockout mice using *Emx1-Cre* (Gorski et al. 2002) and a Bcl11a<sup>Flox</sup> allele in which the exon 4 of Bcl11a was flanked by two loxP sites (Liu et al. 2003; Yu et al. 2012). RNA-seq analyses of the Bcl11a-CKO cortices revealed an efficient deletion of exon 4, and immunohistochemistry showed the absence of the Bcl11a protein in the mutant cortices (Fig. 1H,H',I).

We examined the effect of Bcl11a mutations on cortical neurogenesis. Compared to the littermate control mice, the density of Pax6<sup>+</sup>/Eomes<sup>+</sup> was increased at E12.5 after Bcl11a depletion (1.9-fold,  $P < 0.01$ ) (Fig. 2A–B',D); while the numbers of Pax6<sup>+</sup> cells did not change at E12.5/E13.5, the numbers of Eomes<sup>+</sup> cells were increased among lateral and medial cortex (medial cortex, 1.6-fold of control mice,  $P < 0.01$ ; lateral cortex, 1.6-fold of control mice,  $P < 0.01$ ) (Fig. 2C–C',E). After Bcl11a depletion, RGCs ectopically expressed Eomes, indicating premature neuronal differentiation of cortical RGCs.

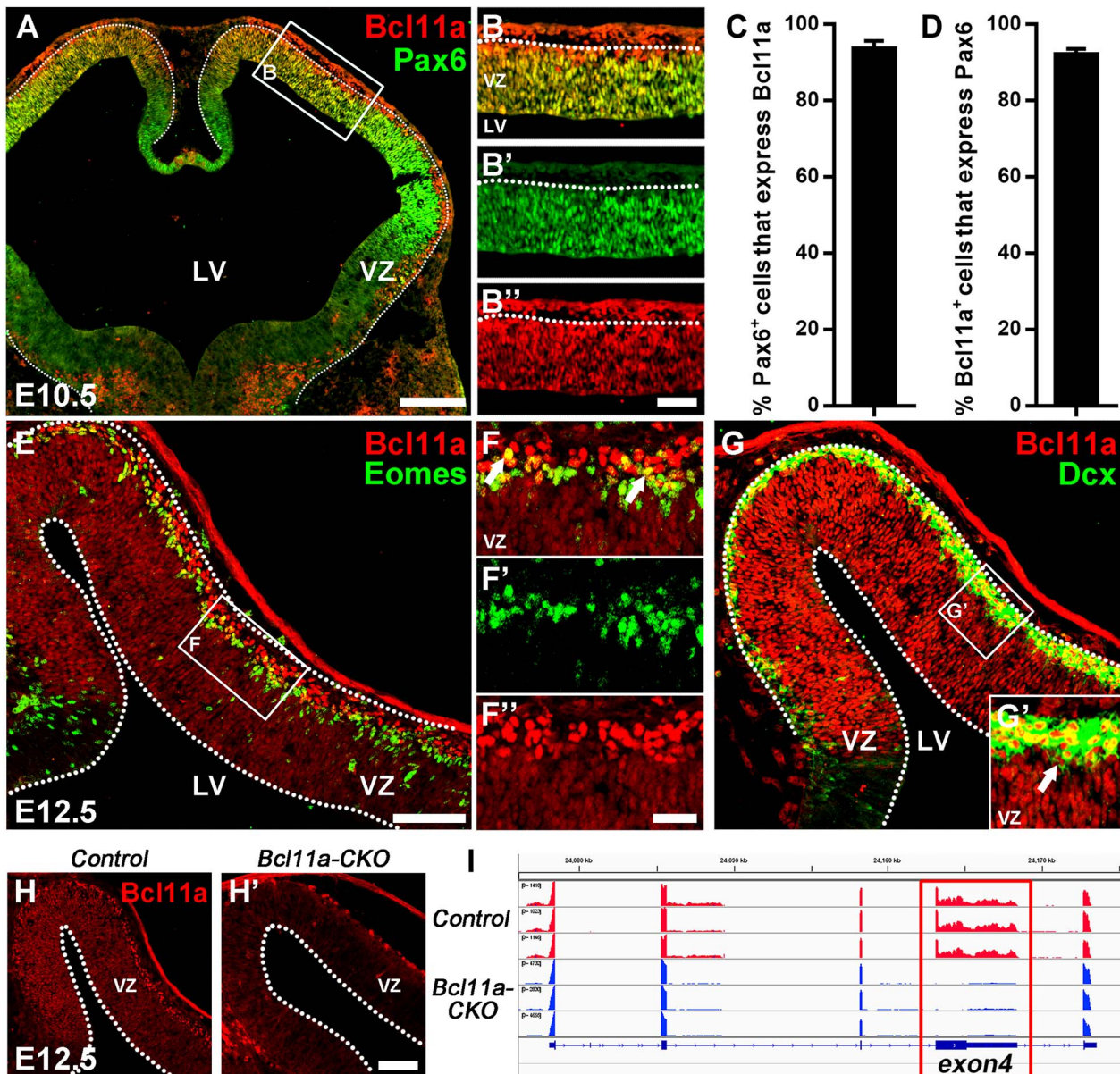


**Fig. 1.** *Bcl11a* is expressed in cortical RGCs at early stages of neurogenesis. (A–B'') *Bcl11a* expression in the mouse cortical VZ at E10.5. Pax6 immunostaining demarcates the VZ. (C, D) Nearly all Pax6<sup>+</sup> cells express *Bcl11a* and vice versa ( $n = 3$ , mean  $\pm$  SEM). (E–F'') *Bcl11a* expression is detected in *Eomes*<sup>+</sup> cortical projection neuron intermediate progenitors (arrows). (G, G') *Bcl11a* is expressed in the *Dcx*<sup>+</sup> immature neurons (arrows). (H, H') *Bcl11a* expression is not detected in the neocortex of *Bcl11a*-CKO mice at E12.5. (I) RNA-Seq data show that the exon 4 (red rectangle) of *Bcl11a* is deleted in the *Bcl11a*-CKO mice. LV, lateral ventricle. White dashed lines indicate the LV and VZ boundaries. Scale bars: 200  $\mu$ m in A for A; 60  $\mu$ m in B'' for B–B''; 100  $\mu$ m in E for E, G; 30  $\mu$ m in F'' for F–F'' and G'; 180  $\mu$ m in H' for H–H'.

We examined the expression of the pan-neuronal marker *Tuj1* and early-born neuron marker *Tbr1* at E13.5. Increased numbers of *Tuj1*<sup>+</sup> and *Tbr1*<sup>+</sup> cells were observed in the mutant cortices than in the control mice (Fig. 2F–G').

Next, we examined whether *Bcl11a* regulates progenitor cell proliferation. Using phosphorylated histone 3 (PH3) antibody staining to label M-phase progenitors, we observed significantly decreased numbers of PH3<sup>+</sup> cells in the VZ of the *Bcl11a*-CKO cortices at E13.5 and E15.5 (Fig. 2H–I'). The density of PH3<sup>+</sup> cells was reduced in

the apical VZ at E13.5 and was reduced in the basal VZ at E13.5/15.5, indicating that the proliferation of both RGCs and IPCs was reduced in the *Bcl11a*-CKO cortices (Fig. 2J).

In the *Bcl11a*-CKO mice, the decreased PH3<sup>+</sup> cortical RGCs suggested that the RGC proliferation was reduced. Meanwhile increased *Eomes*<sup>+</sup> and *Tuj1*<sup>+</sup> cells suggested an accumulation of intermediate progenitors, which might result from a delay in extinguishment of *Eomes* expression or from a premature differentiation of RGCs into IPCs.

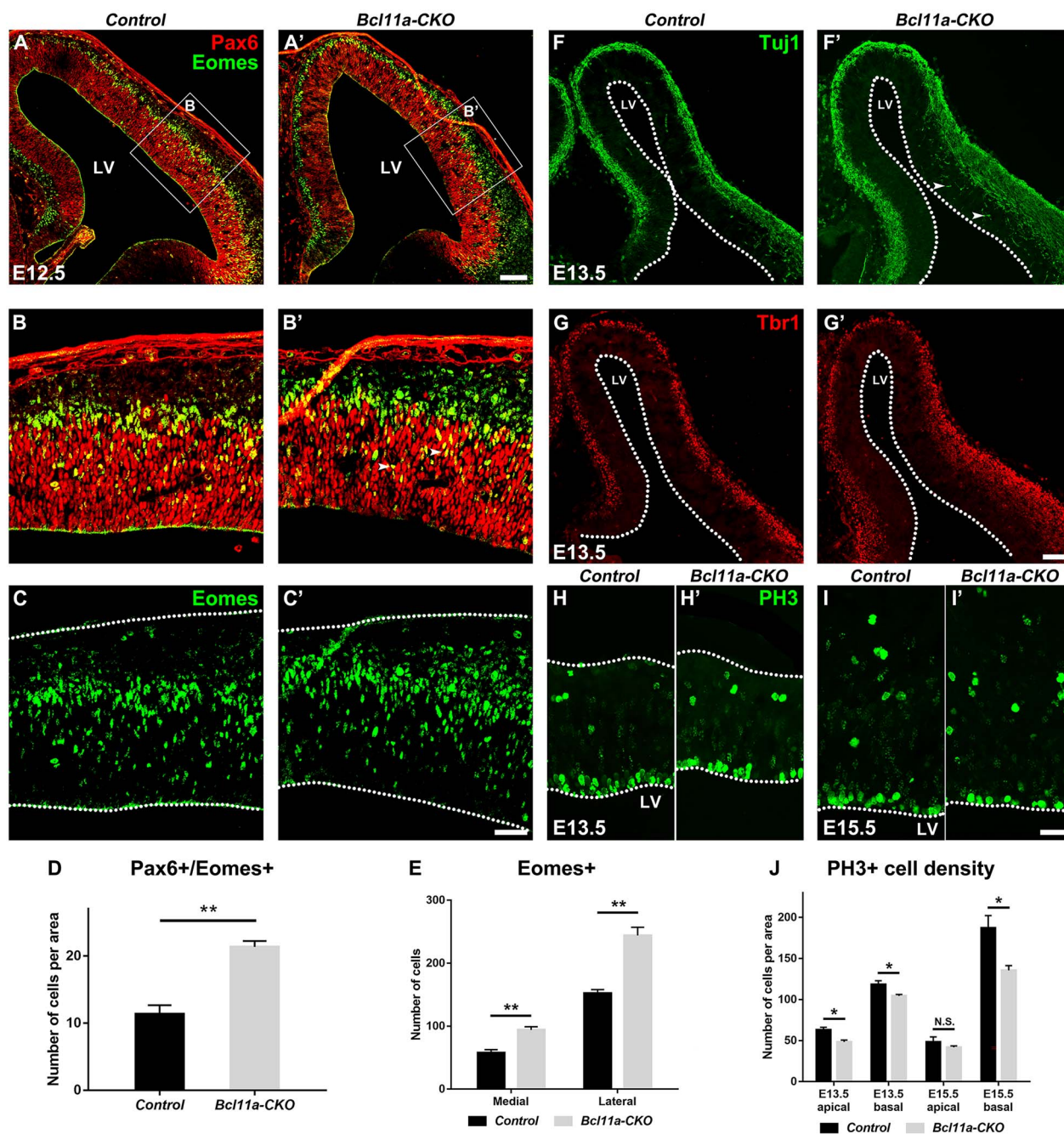


**Fig. 2.** *Bcl11a* promotes cortical RGC proliferation and represses their differentiation. (A–C') More Pax6<sup>+</sup>/Eomes<sup>+</sup> progenitors are present in the *Bcl11a*-CKO mice than in the control mice at E12.5. (D) Quantification of Pax6<sup>+</sup>/Eomes<sup>+</sup> progenitors at E12.5. (Student's t-test, \*\**P* < 0.01, *n* = 3, mean ± SEM). (E) Quantification of Eomes<sup>+</sup> progenitors at E12.5 in medial and lateral cortical area respectively (Student's t-test, \*\**P* < 0.01, *n* = 3, mean ± SEM). (F–G') Increased Tuj1<sup>+</sup> (F and F') and Tbr1<sup>+</sup> (G and G') neurons in the E13.5 *Bcl11a*-CKO cortices. Arrows indicate precocious Tuj1 expression in the progenitors adjacent to the LV. (H–I') PH3<sup>+</sup> cells in the VZ are reduced in the *Bcl11a*-CKO mice compared to the control mice at E13.5 (H–H') and E15.5 (I–I'). (J) Quantification of neurons per area expressing PH3 in the apical and basal VZ at E13.5 and E15.5 (Student's t-test, N.S., not significant, \**P* < 0.05, *n* = 3, mean ± SEM). LV, lateral ventricle. White dashed lines indicate the LV and cortex boundaries. Scale bars: 100 μm in A' for A–A'; 40 μm in C' for B–C'; 100 μm in G' for F–G'; 40 μm in I' for H–I'.

### **Bcl11a and Bcl11b Are Transiently Co-expressed in Migrating Cortical Projection Neurons, and Expression of One Is Increased in Compensation when the Other Gene Is Mutated**

*Bcl11a* and *Bcl11b* are closely related to each other and show approximately 55% similarity of amino

acid sequences. Previous studies showed that *Bcl11b* expression was increased in layer 6 neurons when *Bcl11a* expression was perturbed either by RNAi or by conditional gene knockout (Canovas et al. 2015; Woodworth et al. 2016). It is possible that *Bcl11a* and *Bcl11b* compensate for each other's function in the single knockout mice.

To test this possibility, we performed immunohistochemistry and confirmed that indeed Bcl11b is mainly expressed in postmitotic neurons, but not in progenitor cells in wild-type cortices (Supplementary Fig. S2A–D). We carefully evaluated whether Bcl11a and Bcl11b are co-expressed in the cortical projection neurons and found that they are co-labeled in nearly all of the migrating neurons in the intermediate zone (IZ) and cortical plate (CP) at the mid-stages of cortical neurogenesis (Supplementary Fig. S2E–F’’).

We next investigated how mutations in *Bcl11a* and *Bcl11b* affected the expression of the other. In the control brains, Bcl11b was expressed at high levels in layer 5 neurons and at low levels in layer 6 neurons. Its expression was moderately increased in layer 6 neurons of the *Bcl11a*-CKO brains (Supplementary Fig. S2G,G’). It is possible that Bcl11b compensates for the loss of Bcl11a in layer 6 neurons. We also carefully examined Bcl11b expression in the cortical progenitors in the *Bcl11a*-CKO mice but did not observe increased Bcl11b expression in these cells, indicating Bcl11b is unlikely to compensate for Bcl11a function in the progenitors.

We generated cortex-specific *Bcl11b* knockout mice (*Emx1-Cre*; *Bcl11b*<sup>Flox/Flox</sup>, or *Bcl11b*-CKO) by breeding *Emx1-cre* mice with mice carrying *Bcl11b*<sup>Flox</sup> alleles, in which the exon 4 of *Bcl11b* was flanked by two loxP sites. Some Bcl11b<sup>+</sup> cells remained in the cortices of *Bcl11b*-CKO mice (data not shown), and they were cortical interneurons that originated and migrated from the ventral forebrain. Compared to the control mice, the expression of Bcl11a was increased across all cortical layers in the *Bcl11b*-CKO mice (Supplementary Fig. S2H,H’). These results indicate that the expression of Bcl11a or Bcl11b is increased in compensation in the post-migration cortical projection neurons when the other gene is mutated.

### Reduced Progenitor Proliferation and Precocious Neuronal Differentiation in the *Bcl11a/b*-DCKO Cortices

Previous studies showed that Bcl11b expression was restricted to the postmitotic neurons and ablation of *Bcl11b* resulted in reduced proliferation and depletion of neural stem cells in the hippocampus (Simon et al. 2012). They suggested that dentate gyrus postmitotic neurons could provide feedback signals to regulate the proliferation and maintenance of neural stem cells, which were disrupted after *Bcl11b* depletion. During cortical development, both Bcl11a and Bcl11b were expressed in the postmitotic neurons and could regulate pathfinding or subtype specification, migration, and area identity of cortical projection neurons (Arlotta et al. 2005; Wiegrefe et al. 2015; Greig et al. 2016; Woodworth et al. 2016). It is possible that they function redundantly to control the development of cortical projection neurons, which provide feedback signals to regulate progenitor behaviors. Thus, we performed *Bcl11a/b* double conditional knockout experiments (*Emx1-cre*; *Bcl11a*<sup>Flox/Flox</sup>; *Bcl11b*<sup>Flox/Flox</sup>, or *Bcl11a/b*-DCKO)

to investigate whether Bcl11a and Bcl11b together regulate progenitor proliferation, maintenance, and differentiation in the developing cortex.

While the density of Pax6<sup>+</sup> cells and the VZ thickness were not significantly affected in the *Bcl11a*-CKO and *Bcl11b*-CKO mice, the decreased number of the Pax6<sup>+</sup> cells in E15.5 double mutant cortices (40.7% of control mice,  $P < 0.001$ ) led to significantly reduced thickness of the VZ (Fig. 3A–E). Quantification of the numbers of the PH3<sup>+</sup> cells in the VZ and SVZ revealed much fewer PH3<sup>+</sup> cells in the *Bcl11a/b*-DCKO mice (E13.5, 76.6% of control mice,  $P < 0.01$ ; E15.5, 44.5% of control mice,  $P < 0.01$ ), indicating reduced progenitor cell proliferation in the absence of both *Bcl11a* and *Bcl11b* (Fig. 3F–H).

The reduced progenitor cell proliferation in the *Bcl11a/b*-DCKO mice could be due to either accelerated mitotic cell cycle exit or prolonged cell cycle length. We performed cell cycle quit fraction analyses and found no significant differences in the proportion of progenitors quitting the cell cycle at E13.5 or E15.5 (data not shown). To examine the cell cycle length, we employed pulse-chase of BrdU to label S-phase precursors, followed by an injection of EdU incorporated into proliferative cells 1.5 h later. We collected the brains 0.5 h after the EdU injection and utilized the single labeling cell (BrdU<sup>+</sup> EdU<sup>-</sup>) numbers during the internal period to estimate the cell cycle length. The cell cycle length was calculated using a published method (Martynoga et al. 2005; Seuntjens et al. 2009; Wang et al. 2016). It was significantly prolonged in the *Bcl11a/b*-DCKO precursors at E13.5 and E15.5 (E13.5, 1.27-fold of control,  $P < 0.05$ ; E15.5, 2.7-fold of control,  $P < 0.001$ ), which might partially contribute to the defective proliferation of the mutant mice (Fig. 3I–N).

Precocious differentiation of cortical progenitors was observed in the *Bcl11a*-CKO mice (Fig. 2). We investigated whether lack of both *Bcl11a* and *Bcl11b* would exacerbate the phenotype. The numbers of Eomes<sup>+</sup> cells were increased in the *Bcl11a/b*-DCKO mice at E12.5 and E13.5 compared to their respective control mice (E12.5, 2.0-fold of control,  $P < 0.001$ ; E13.5, 2.1-fold of control,  $P < 0.001$ ) (Fig. 4A–F’). Compared to the *Bcl11a*-CKO cortices, the number of Eomes<sup>+</sup> cells was slightly increased in the *Bcl11a/b*-DCKO cortices but did not reach a statistical significance (Fig. 4G, left). At E15.5, the numbers of the Eomes<sup>+</sup> intermediate progenitors in the *Bcl11a/b*-DCKO mice were not significantly different from those in the control mice (Fig. 4E–G).

Consistent with increased numbers of Eomes<sup>+</sup> cells at E12.5 and E13.5, we observed more Tbr1<sup>+</sup> neurons in the *Bcl11a/b*-DCKO mice at the same stages (Fig. 4H–K’). However, the number of neurons with strong Tbr1 expression was reduced in the *Bcl11a/b*-DCKO cortices at E15.5 (Fig. 4L–M’). At P0, Tbr1 expression was virtually invisible in the motor and somatosensory cortices of the *Bcl11a/b*-DCKO mice (Fig. 4N–O’). These results indicate that *Bcl11a* and *Bcl11b* together regulate RGC proliferation and progenitor differentiation in the developing cerebral cortex.



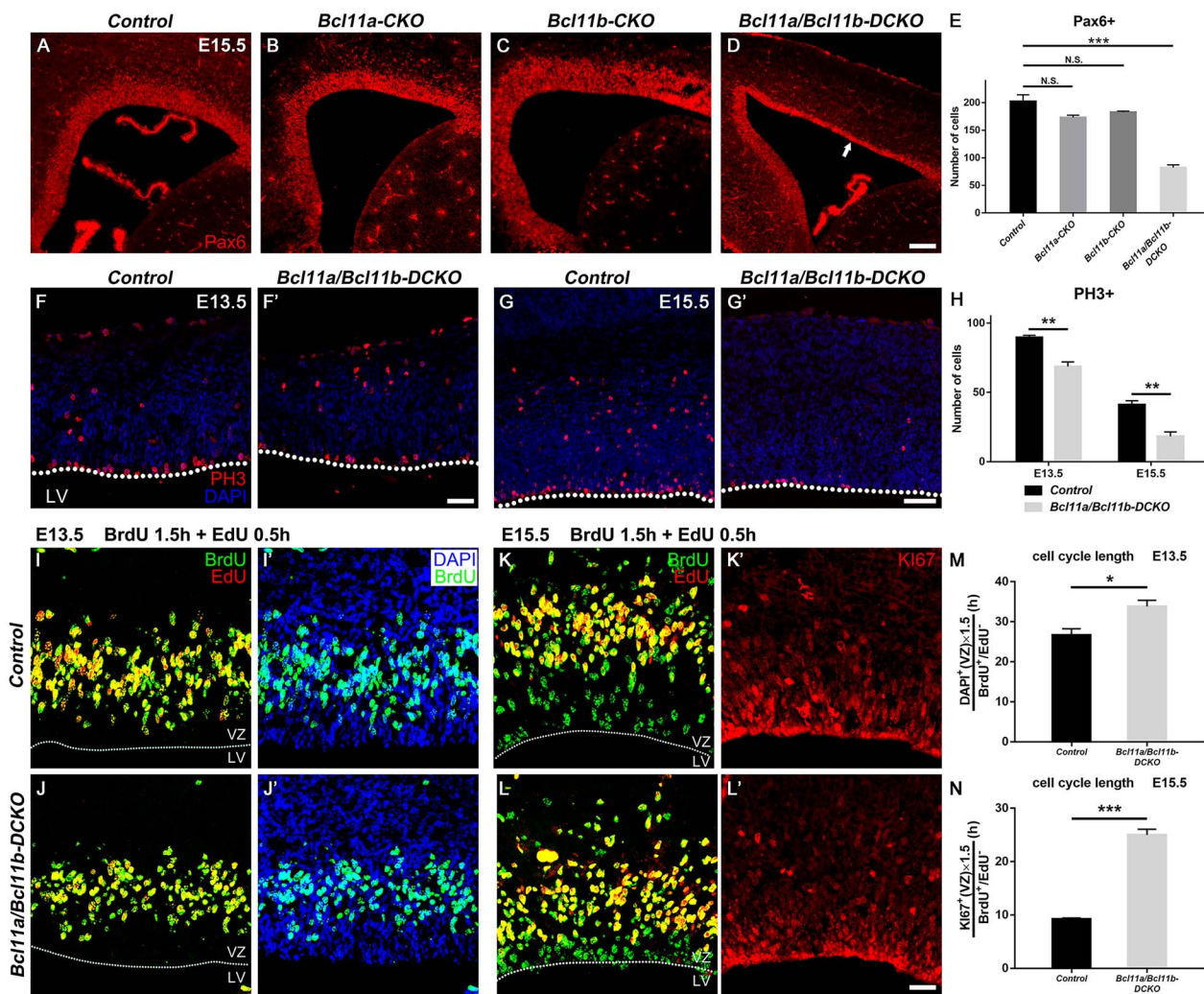


**Fig. 3.** Depletion of cortical RGCs in *Bcl11a/b-DCKO*. (A–D) Pax6 expression in VZ in control (A), *Bcl11a-CKO* (B), *Bcl11b-CKO* (C), and *Bcl11a/b-DCKO* mice (D, arrow) at E15.5. (E) The numbers of Pax6<sup>+</sup> cells in the cortical VZ of *Bcl11a/b-DCKO* are significantly fewer than those in the controls at E15.5 (one-way ANOVA, followed by a Tukey HSD post hoc test; N.S., not significant, \*\*\**P* < 0.001, *n* = 3, mean ± SEM). (F–G') Representative images of PH3<sup>+</sup> cells in the VZ/SVZ of controls and *Bcl11a/b-DCKO* at E13.5 (F and F') and E15.5 (G and G'), respectively. (H) The numbers of PH3<sup>+</sup> cells in the cortical VZ are significantly fewer in the *Bcl11a/b-DCKO* mice than those in the control mice (Student's *t*-test, \*\**P* < 0.01, *n* = 3, mean ± SEM). (I–L') Representative images of BrdU, EdU, and DAPI stainings in the controls and *Bcl11a/b-DCKO* at E13.5 (I–J') and BrdU, EdU, and Ki67 stainings in the controls and *Bcl11a/b-DCKO* at E15.5 (K–L'). (M) Quantification of cell cycle length index DAPI<sup>+</sup>(VZ)/BrdU<sup>+</sup> EdU<sup>-</sup> in the progenitors as indicated in (I–J') (Student's *t*-test, \**P* < 0.05, *n* = 3, mean ± SEM). (N) Quantification of cell cycle length index Ki67<sup>+</sup>(VZ)/BrdU<sup>+</sup> EdU<sup>-</sup> in the progenitors as indicated in (K–L') (Student's *t*-test, \*\*\**P* < 0.001, *n* = 3, mean ± SEM) LV, lateral ventricle; VZ, ventricular zone. White dashed lines indicate the LV boundaries. Scale bars: 200 μm in D for A–D; 100 μm in F' for F–F'; 160 μm in G' for G–G'; 30 μm in L' for I–L'.

### Lack of *Bcl11a* and *Bcl11b* Leads to Decreased Cortical Thickness and Increased Cell Death of Cortical Neurons

The *Bcl11a/b-DCKO* mice die at birth. To determine the long-term effect of mutating both genes on cortical development, we examined the P0 brains from the control, the *Bcl11a-CKO*, the *Bcl11b-CKO*, and the *Bcl11a/b-DCKO* mice. Nissl staining showed the decreases in cortical thickness and enlarged lateral ventricles in the *Bcl11a/b-DCKO* mice (Fig. 5A–E). The corpus callosum was normal size in the control and *Bcl11b-CKO* mice, it was reduced in the *Bcl11a-CKO* mice, and absent in the *Bcl11a/b-DCKO* mice (Fig. 5A,B,D).

We examined the numbers of cortical neurons by performing immunohistochemistry for NeuN, a

pan-neuronal marker. Compared to the control mice, the numbers of NeuN<sup>+</sup> cells in the cortical plates of the *Bcl11a-CKO* and *Bcl11a/b-DCKO* mice were significantly reduced (Fig. 5F–J).

To investigate whether loss of *Bcl11a/b* affects the production and the laminar position of cortical neurons, we injected BrdU into pregnant females at E13.5 and collected the brains at P0. The total numbers of BrdU<sup>+</sup> cells were not significantly affected in the *Bcl11a-CKO* or *Bcl11b-CKO* mice, but only two-thirds of BrdU<sup>+</sup> cells (67.12% of control brains, *P* < 0.01) were present in the cortical plates of the *Bcl11a/b-DCKO* mice at P0 (Fig. 5K–O). We divided the IZ and CP into 10 bins and quantified the density of BrdU<sup>+</sup> cells in each bin (Supplementary Fig. S3A–D'). While BrdU<sup>+</sup> cells labeled at E13.5 preferred

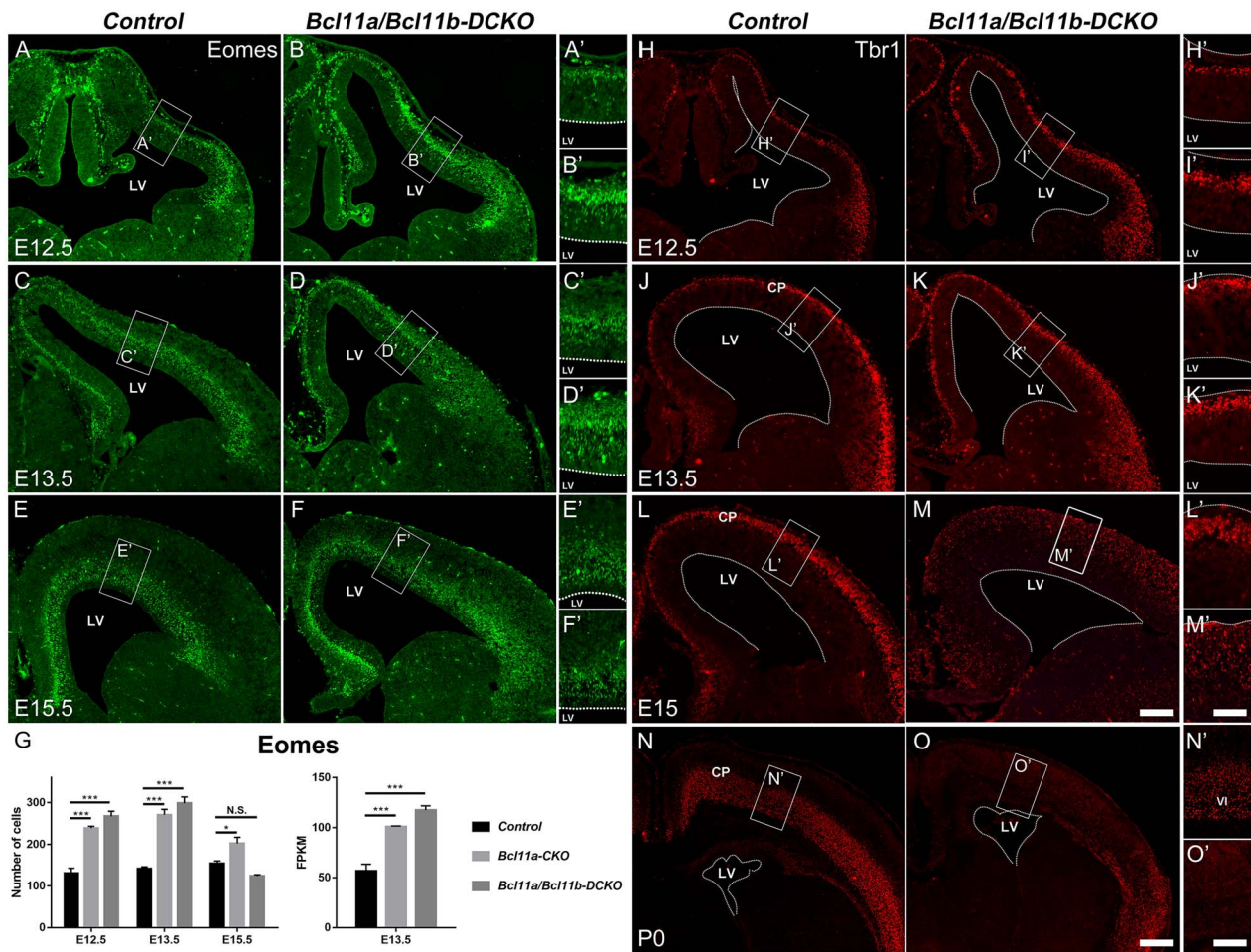


**Fig. 4.** The premature differentiation of cortical projection neuron intermediate progenitors in *Bcl11a/b-DCKO*. (A–F) In the absence of *Bcl11a* and *Bcl11b*, *Eomes* expression in SVZ is remarkably increased at E12.5 (A–B) and E13.5 (C–D) in *Bcl11a/b-DCKO* compared to the control brains. (G) Quantification of the numbers of *Eomes*<sup>+</sup> cells in the cortices (left) and the FPKM values of *Eomes* gene expression based on RNA-seq data at E13.5 (right) (Student’s t-test, N.S., not significant, \**P* < 0.05, \*\*\**P* < 0.001, *n* = 3, mean ± SEM). (H–O’) Expression of early-born neuron marker *Tbr1* in the control and *Bcl11a/b-DCKO* cortices at E12.5 (H–I’), E13.5 (J–K’), E15 (L–M’), and at P0 (N–O’). (H–K’) Compared to the control cortices, more neurons in *Bcl11a/b-DCKO* express *Tbr1* at E12.5 and E13.5. (L–M’) Numbers of *Tbr1*<sup>+</sup> cells appear increased at E15, but the expression in each cell is lower than the control. (N–O’) Compared to the control brains at P0, fewer cortical neurons express *Tbr1* in the dorsal cortex of *Bcl11a/b-DCKO*. LV, lateral ventricle; CP, cortical plate. White dashed lines indicate the LV boundaries. Scale bars: 200 μm in M for A–F and H–M; 100 μm in M’ for A’–F’ and H’–M’; 300 μm in O for N,O; 150 μm in O’ for N’–O’.

to distribute among bins 3–7 in the control or single CKO brains, they were evenly distributed in the *Bcl11a/b-DCKO* brains. Compared to the BrdU<sup>+</sup> cortical cells in the control and single CKO brains, more BrdU<sup>+</sup> cells were ectopically distributed in bins 8–10 just above the SVZ (Supplementary Fig. S3E), indicating abnormal neuronal migration and laminar position after *Bcl11a/b* depletion. Taken together, these results indicated that the production, migration, and laminar position of cortical projection neurons were affected after *Bcl11a/b* depletion.

We next determined whether mutations in *Bcl11a* and *Bcl11b* led to changes in cell viability. Staining of activated Caspase-3 showed a significant increase in cell death in the *Bcl11a-CKO* at P0, and there was a 5-fold (*P* < 0.001) increase of apoptosis in the *Bcl11a/b-DCKO* cortices (Fig. 5P–T). The increased Caspase-3<sup>+</sup> cells were present both in the VZ/SVZ and the cortical plate. Thus, *Bcl11a* and *Bcl11b* are required for the survival of the cortical progenitors and projection neurons.

### ***Bcl11a* and *Bcl11b* Jointly Regulate Subtype Specification and Differentiation of Multiple Subtypes of Cortical Projection Neurons**

It was reported that *Bcl11a* regulated the balance between distinct projection neuron subtypes in deep cortical layers (Woodworth et al. 2016). Loss of *Bcl11a* function resulted in increased numbers of layer V subcerebral neuron development in the sensory cortex at the expense of corticothalamic neurons and deep-layer callosal neurons (Woodworth et al. 2016). Given the co-expression of *Bcl11a* and *Bcl11b* in migration neurons when both deep-layer and upper-layer cortical projection neurons are generated, the increased expression of *Bcl11a* in the layer VI neurons of the *Bcl11b-CKO* mice, and the increased expression of *Bcl11b* in cortical neurons in the *Bcl11a-CKO* mice, it is possible that these two proteins function redundantly in regulating projection neuron subtype specification and differentiation. To test this possibility, we performed in situ hybridization on E15

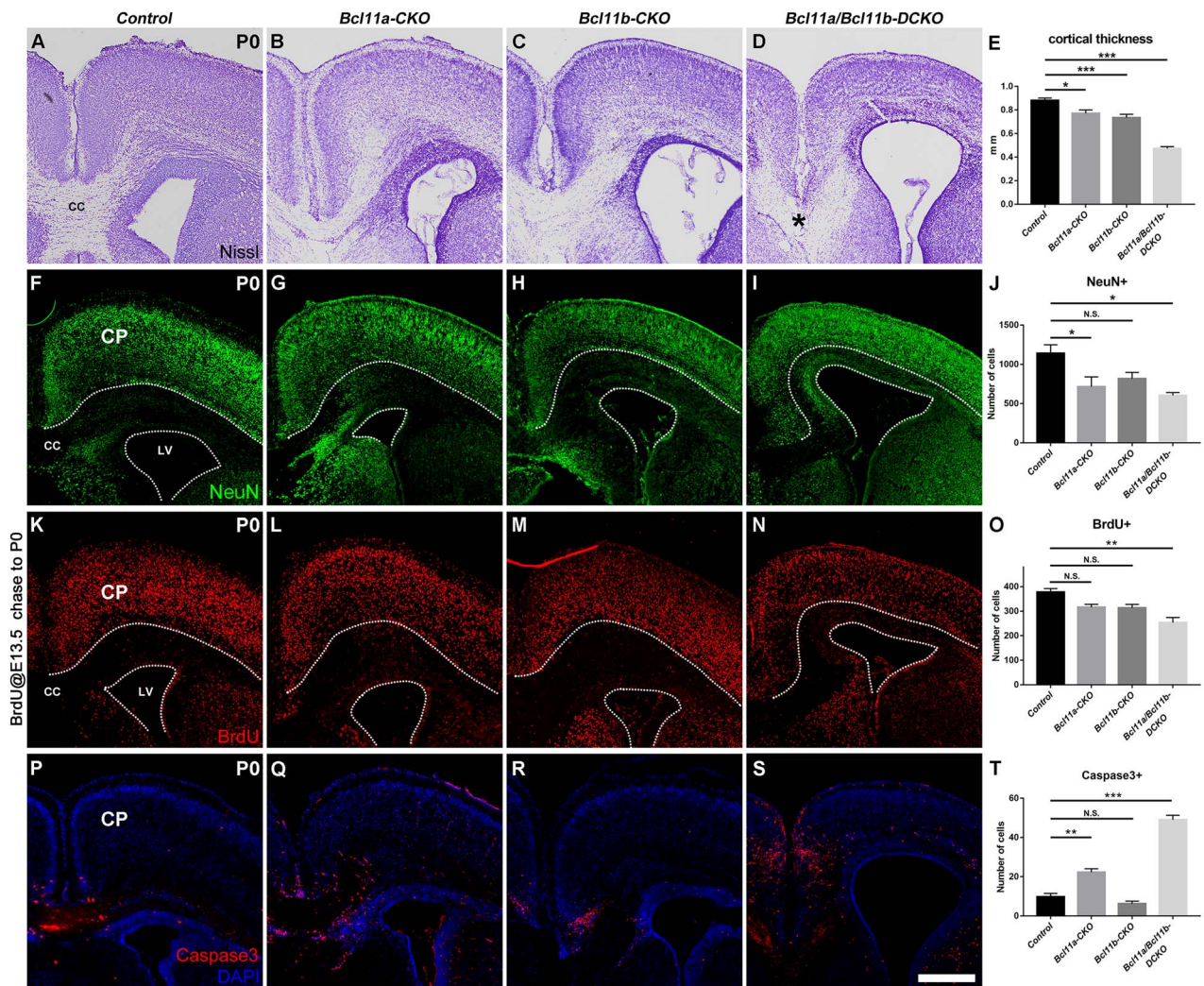


**Fig. 5.** Defects of cortical structure, production, differentiation, and cell death in the cortices of *Bcl11a/b*-DCKO mice. (A–D) Nissl staining of cortices in the control mice (A) and conditional knockout mice (B–D). Note the disorganization of laminar structure and loss of corpus callosum in *Bcl11a/b*-DCKO (asterisk in D). (E) Measurement of the cortical thickness at P0. (one-way ANOVA, followed by a Tukey HSD post hoc test; \* $P < 0.05$ , \*\*\* $P < 0.001$ ,  $n = 6$ , mean  $\pm$  SEM). (F–I) Immunostaining of pan-neuronal marker NeuN at P0. (J) Quantification of NeuN<sup>+</sup> neurons in the cortical plate at P0 (one-way ANOVA, followed by a Tukey HSD post hoc test; N.S., not significant, \* $P < 0.05$ ,  $n = 3$ , mean  $\pm$  SEM). (K–N) BrdU is administered at E13.5; BrdU<sup>+</sup> cells in the cortices are analyzed at P0. (O) Quantification of the BrdU<sup>+</sup> neurons in the cortical plates at P0 (one-way ANOVA, followed by a Tukey HSD post hoc test; N.S., not significant, \*\* $P < 0.01$ ,  $n = 3$ , mean  $\pm$  SEM). (P–S) Immunostaining of cell death marker Cleaved Caspase-3 (red) at P0. (T) Numbers of Caspase-3<sup>+</sup> cells are significantly higher in the *Bcl11a/b*-DCKO than in the controls (one-way ANOVA, followed by a Tukey HSD post hoc test; N.S., not significant, \*\* $P < 0.01$ , \*\*\* $P < 0.001$ ,  $n = 3$ , mean  $\pm$  SEM). CP, cortical plate; CC, corpus callosum; LV, lateral ventricle. White dashed lines indicate the CP and LV boundaries. Scale bars: 400  $\mu$ m in S for A–D, F–I, K–N, and P–S.

brain sections. Compared to the control mice, the expression of early pan-neuronal genes including *Cnr1*, *Plk2*, *Shtn1*, and *Dync1i1* were reduced in the cortices of both *Bcl11a*-CKO and *Bcl11b*-CKO mice, but their expression was absent in the *Bcl11a/b*-DCKO cortices (Fig. 6A–B'', Supplementary Fig. S4A–B''), which is consistent with the RNA-seq data (Fig. 6F,G, Supplementary Fig. S4F,G), suggesting that *Bcl11a* and *Bcl11b* redundantly regulate the differentiation of cortical projection neurons.

We performed RNA-seq analyses of the control, *Bcl11a*-CKO, *Bcl11b*-CKO, and *Bcl11a/b*-DCKO cortices at P0 and found that the expression of many subtype-specific genes was affected in the single or double mutant mice. We validated the RNA-seq results by performing

in situ hybridization or immunohistochemistry. RNA-seq analysis indicated the misregulated expression of genes that mark callosal neurons, including *Satb2* and *Cux1* (Fig. 6I,J). In situ hybridization confirmed that their expression was reduced in the cortices of the *Bcl11a*-CKO, *Bcl11b*-CKO, and the *Bcl11a/b*-DCKO mice (Fig. 6D–E''). The decreased *Cux1* expression was more severe in the *Bcl11a/b*-DCKO mice than in the *Bcl11a*-CKO and the *Bcl11b*-CKO mice. RNA-seq analysis similarly revealed reduced expression for layer IV granular neuron gene *Rorb* in the P0 *Bcl11a*-CKO, *Bcl11b*-CKO mice (Fig. 6H), which was exacerbated in the *Bcl11a/b*-DCKO cortices. In situ hybridization data confirmed the RNA-seq analysis results (Fig. 6C–C'').

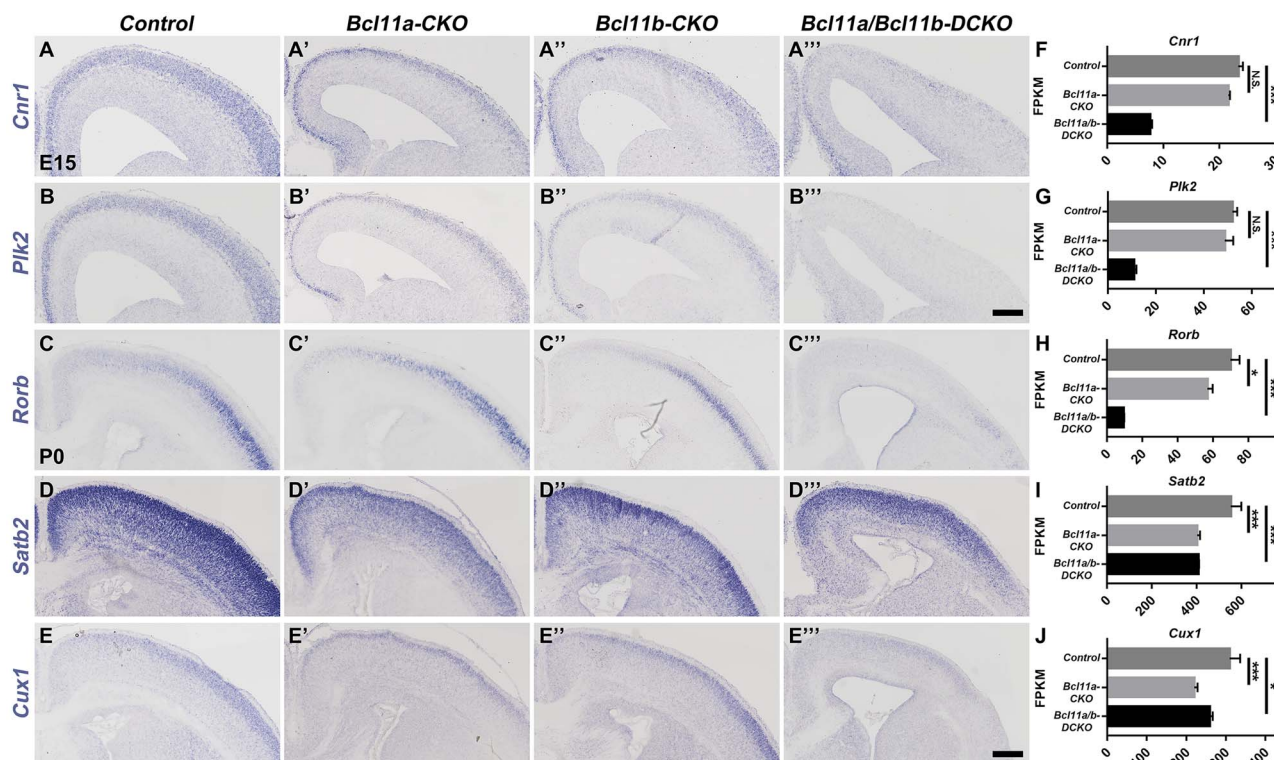


**Fig. 6.** Expression of some upper-layer neuronal genes is reduced after *Bcl11a* and *Bcl11b* depletion. (A–E''') In situ hybridization results show severely reduced expression of the pan-neuronal genes *Cnr1* (A–A''') and *Plk2* (B–B''') in the cortices of *Bcl11a/b*-DCKO mice at E15. (C–E''') Expression of layer IV projection neurons gene *Rorb* is missing, whereas *Satb2* and *Cux1* show reduced expression in the *Bcl11a/b*-DCKO mice at P0. (F–J) The FPKM values of the genes based on RNA-seq data at the ages corresponding to the in situ experiments (Student's *t*-test, N.S., not significant, \**P* < 0.05, \*\*\**P* < 0.001, *n* = 3, mean ± SEM). Scale bars: 200 μm in B'''' for A–B''''; 300 μm in E'''' for C–E''''.

We examined whether and how the genes associated with deep-layer neuronal subtypes were affected in the mutant mice. A previous study (Woodworth et al. 2016) reported that layer V subcerebral neurons expanded at the expense of layer VI corticothalamic and deep-layer callosal neurons in the *Bcl11a*-CKO mice. Our RNA-seq analysis, in situ hybridization, and immunohistochemistry confirmed the increased expression of some layer V subcerebral neuron genes such as *Otx1* (Supplementary Fig. S4C–C',H) and the decreased expression of layer VI corticothalamic neuronal genes such as *Tle4* (Fig. 7A,A',G), *Ppp1r1b* (Fig. 7B,B',H), and *Foxp2* (Supplementary Fig. S4E,E',J), in the *Bcl11a*-CKO mice. However, our analyses revealed that the expression of these genes and of many other genes associated with layer V subcerebral, layer VI corticothalamic, and subplate neurons was severely reduced or almost absent in the *Bcl11a/b*-DCKO cortices (Fig. 7 and Supplementary Fig. S4). The dramatic reduction or loss of molecular characteristics associated with deep-layer corticofugal neurons in the *Bcl11a/b*-DCKO indicates that these two genes redundantly promote the subtype identities of corticofugal neurons.

In summary, both *Bcl11a* and *Bcl11b* functions are required for the differentiation of cortical projection neurons, and they redundantly promote neuronal

subtype identities, especially for the layer V subcerebral and layer VI corticothalamic neurons.

### Major Cortical Axon Tracts Are Defective in the *Bcl11a/b*-DCKO Mice

Next, we examined whether *Bcl11a* and *Bcl11b* jointly regulated the axonal projections of the cortical excitatory neurons. To this end, we bred IS reporter mice (*Rosa-CAG-LSLFrtdTomato-Frt-EGFP*) (He et al. 2016; Li et al. 2021) with *Emx1-cre* mice to directly visualize the axons of cortical neurons. In the control (*Emx1-cre*; IS) mice, tdTomato<sup>+</sup> corticothalamic axons from layer VI neurons, subcerebral axons including the corticospinal tract axons from layer V neurons, and callosal axons were easily identified (Fig. 8A–A'). In the *Bcl11a/b*-DCKO; IS mice, the corticothalamic axons were absent (Fig. 8A–D',H–H', Supplementary Fig. S5B–B'''). The cerebral peduncle axons were reduced in the *Bcl11b*-CKO; IS mice and no tdTomato<sup>+</sup> axons were observed extending to the cerebral peduncle or reaching the spinal cord in the *Bcl11a/b*-DCKO; IS mice (Fig. 8A–D',E–G', Supplementary Fig. S5C–D'''). Similarly, the callosal axons failed to enter the corpus callosum and to cross the midline in the *Bcl11a/b*-DCKO; IS mice (Supplementary Fig. S5A–A'''). The much more severe defects in the *Bcl11a/b*-DCKO; IS

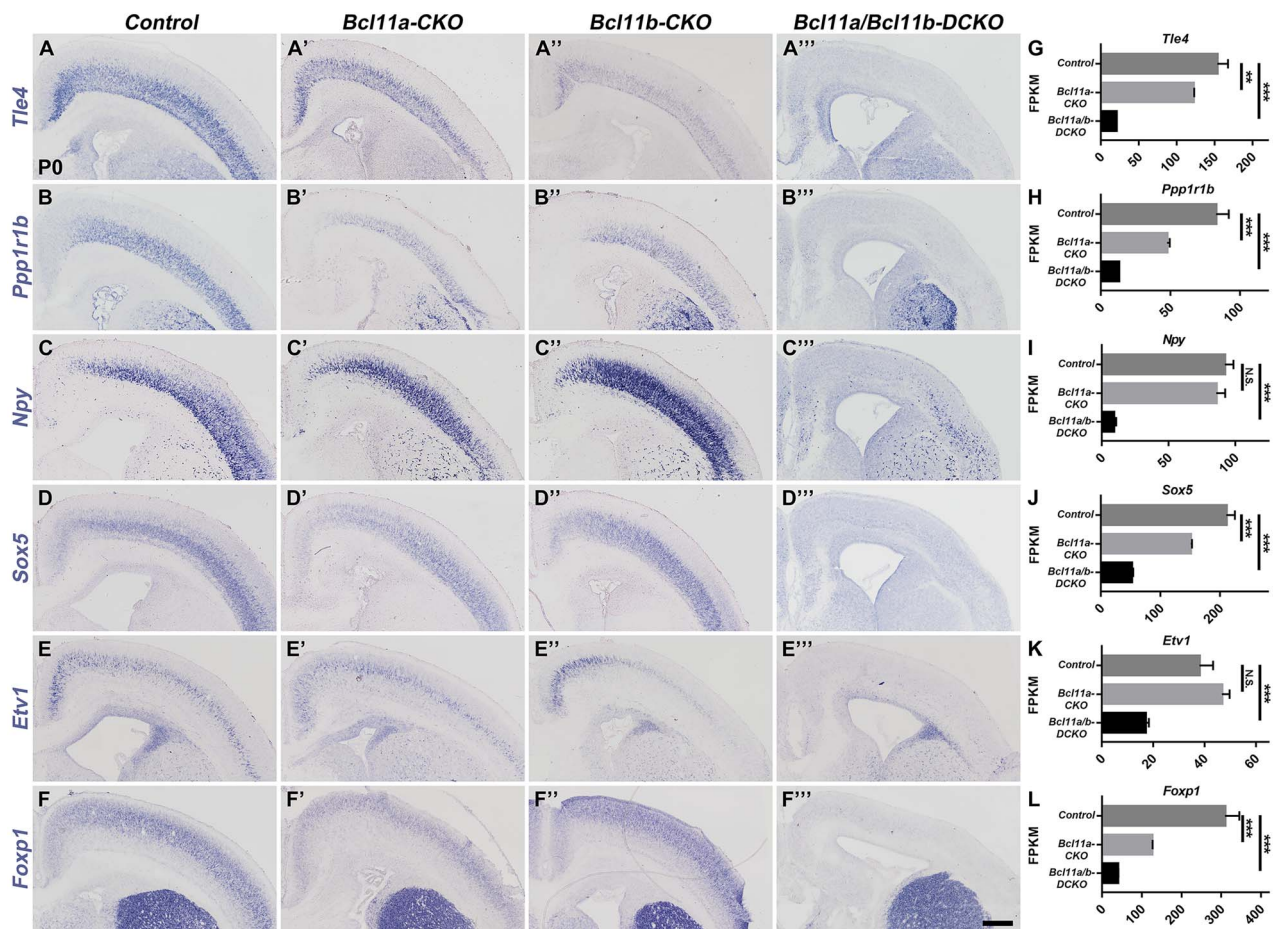


**Fig. 7.** Most of the deep-layer projection neuron marker genes are not expressed in the *Bcl11a/b*-DCKO cortices. (A–D'') In situ hybridization shows that expression of the corticothalamic neuron and subplate genes *Tle4*, *Ppp1r1b*, *Npy*, and *Sox5* is almost absent in *Bcl11a/b*-DCKO cortices at P0. (E–F'') Some of the specific projection neuron genes confined in layer V, such as *Etv1* and *Foxp1*, show reduced expression in the *Bcl11a/b*-DCKO cortices. (G–L) The FPKM values of the genes based on RNA-seq data at P0 (Student's t-test, N.S., not significant, \*\* $P < 0.01$ , \*\*\* $P < 0.001$ ,  $n = 3$ , mean  $\pm$  SEM). Scale bars: 300  $\mu$ m in F'' for A–F''.

mice than the single mutant mice indicate that *Bcl11a* and *Bcl11b* redundantly regulate the development of all major cortical axon tracts, including the corticothalamic, layer V subcerebral, and callosal axons.

### ***Bcl11a* Promotes RGC Proliferation and Inhibits Differentiation through Repressing *Nr2f1* Expression**

We sought to uncover the possible mechanism for *Bcl11a* and *Bcl11b* to regulate cortical neurogenesis. *Bcl11* proteins were initially isolated through their interactions with Coup-Tf family nuclear receptors (also known as *Nr2f* nuclear receptors), and *Bcl11a* can also function as a transcriptional repressor independent of Coup-Tf family members (Avram et al. 2002; Simon et al. 2020). Recently, the protein motifs in the *Bcl11a* protein that mediate the interaction with members of the *Nr2e/f* family transcription factors have been identified (Chan et al. 2013).

*Nr2f1* plays essential roles in promoting differentiation and repressing proliferation of RGCs in the cortex (Faedo et al. 2008; Borello et al. 2014). The increased production of Eomes<sup>+</sup> progenitors, and Tuj1<sup>+</sup> and Tbr1<sup>+</sup> neurons in the *Bcl11a*-CKO and *Bcl11a/b*-DCKO cortices was similar to

the cortices when *Nr2f1* was overexpressed (Faedo et al. 2008). We tested whether *Nr2f1* expression was affected in the *Bcl11a*-CKO and *Bcl11a/b*-DCKO cortices using in situ hybridization. In the control cortices, the expression of *Nr2f1* in VZ at E12.5 exhibits caudal ventral high–rostral dorsal low gradient, consistent with a previous report (Borello et al. 2014). At E12.5 and E15.5, the expression of *Nr2f1* in the VZ/SVZ was elevated and shifted dorsally and rostrally in both the *Bcl11a*-CKO and *Bcl11a/b*-DCKO cortices, with the increased expression level and dorsal shift being more significant in the *Bcl11a/b*-DCKO cortices (Fig. 9B–C''). At P0, *Nr2f1* expression in the cortical plate was reduced in the *Bcl11a*-CKO cortices (Fig. 9K–K''), which is consistent with a previous study that showed decreased *Nr2f1* expression in the *Bcl11a*-CKO cortices as area identity shifts (Greig et al. 2016). Our RNA-seq analysis confirmed the increased *Nr2f1* expression in the *Bcl11a*-CKO and *Bcl11a/b*-DCKO cortices at early stage and the decreased *Nr2f1* expression at later stage (Fig. 9H–J).

We performed a CUT&Tag experiment using a *Bcl11a* antibody and found that *Bcl11a* binds to the *Nr2f1* gene locus (Fig. 9A), suggesting that it may directly inhibit *Nr2f1* expression in the developing cortex.

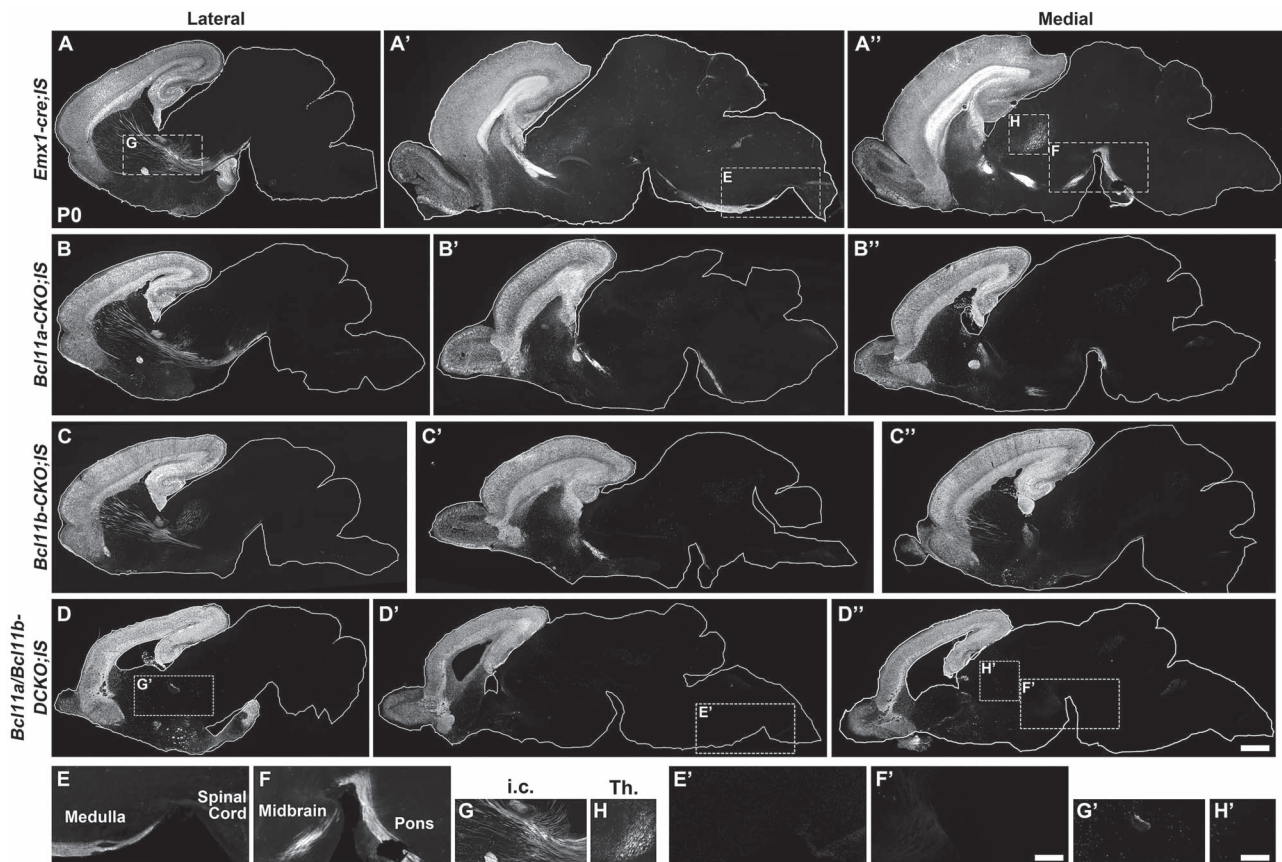


**Fig. 8.** Defects of deep-layer projection neuron axonal projections in *Bcl11a/b-DCKO* at P0. (A–D'') Sagittal sections show tdTomato staining in control (*Emx1-cre*; IS) brains (A–A''), *Bcl11a-CKO*; IS brains (B–B''), *Bcl11b-CKO*; IS brains (C–C''), and *Bcl11a/b-DCKO*; IS brains (D–D''). (E, F, E', F') tdTomato<sup>+</sup> axons extend through midbrain, pons, and medulla towards spinal cord in the control brains (E and F), whereas these axons are absent in both *Bcl11a/b-DCKO* (E' and F') and *Bcl11b-CKO* mice (C–C''). (G, G') tdTomato<sup>+</sup> axons are present in the internal capsule of control mice (G) but rare in *Bcl11a/b-DCKO* brains (G'). (H, H') tdTomato<sup>+</sup> corticothalamic axons are present in the control brains but absent in the thalamus of *Bcl11a/b-DCKO* brains. i.c., internal capsule; Th., thalamus. Scale bars: 600  $\mu\text{m}$  in D'' for A–D''; 300  $\mu\text{m}$  in F' for E–F and E'–F'; 360  $\mu\text{m}$  in H' for G–H and G'–H'.

Compared to the *Bcl11a-CKO* cortices, *Nr2f1* expression was further derepressed in the *Bcl11a/b-DCKO* (Fig. 9B–G'). Since *Bcl11b* expression is restricted to postmitotic neurons in both control and *Bcl11a-CKO* cortices, it could not compensate *Bcl11a* function in RGCs and progenitors to repress *Nr2f1* expression. We showed above that *Bcl11a/b* were required to specify the deep layer neurons which might provide feedback signaling to RGCs. Loss of deep layer neurons in the *Bcl11a/b-DCKO* cortices would disrupt the feedback signaling and result in further increase of *Nr2f1* expression.

### Precocious Neurogenesis to Gliogenesis Switch in the Absence of *Bcl11* Genes

At the end of cortical neurogenesis, cortical RGCs undergo a major switch to generate cortical oligodendrocytes and astrocytes (Li et al. 2021). We investigated whether the neurogenesis to gliogenesis switch was affected in the knockout mice. During normal development, the expression of *Aldh111* and *Egfr*, genes associated with gliogenesis, is detected in the cortical VZ/SVZ around E16.5 (Beattie et al. 2017; Zhang, Mennicke, et al. 2020; Li et al. 2021). *Aldh111*<sup>+</sup> cells were observed in the cortical VZ/SVZ in the E15.5

*Bcl11a-CKO* and the *Bcl11a/b-DCKO* mice, whereas they were not observed in the controls at the same gestation age (Fig. 10A–A''). Further, more *Egfr*<sup>+</sup> cells were present in the cortical VZ/SVZ at E16 in the *Bcl11a-CKO* and the *Bcl11a/b-DCKO* mice (Fig. 10C–C''). Another glial marker, *Gfap*, showed increased expression in the VZ/SVZ of both the *Bcl11a-CKO* and the *Bcl11a/b-DCKO* mice at E16 (Fig. 10B–B'').

During early stage the cortical RGCs produce *Eomes*<sup>+</sup> IPCs to give birth to projection neurons; during later stage they produce *Olig2*<sup>+</sup>/*Egfr*<sup>+</sup> IPCs to produce olfactory bulb interneurons, cortical oligodendrocytes, and astrocytes. To further study the possible premature gliogenesis, we investigated the *Olig2*, *Egfr*, *Sox10*, *Aldh111* expression in the *Bcl11a/b-DCKO* mice. We identified the glia population as follows: glial progenitors, *Olig2*<sup>+</sup>/*Egfr*<sup>+</sup>; oligodendrocytes, *Sox10*<sup>+</sup>; astrocytes, *Aldh111*<sup>+</sup> cells in the CP. In the *Bcl11a/b-DCKO* mice, we observed increased *Olig2*<sup>+</sup>/*Egfr*<sup>+</sup> IPCs at E16 (Fig. 10D–G'',L), slightly but not significantly increased density of *Sox10*<sup>+</sup> oligodendrocytes and significantly increased density of *Aldh111*<sup>+</sup> astrocytes at P0 (Fig. 10H–K'',M,N). These results indicate a precocious gliogenesis at late gestation stage in the *Bcl11a-CKO* and *Bcl11a/b-DCKO* mice.

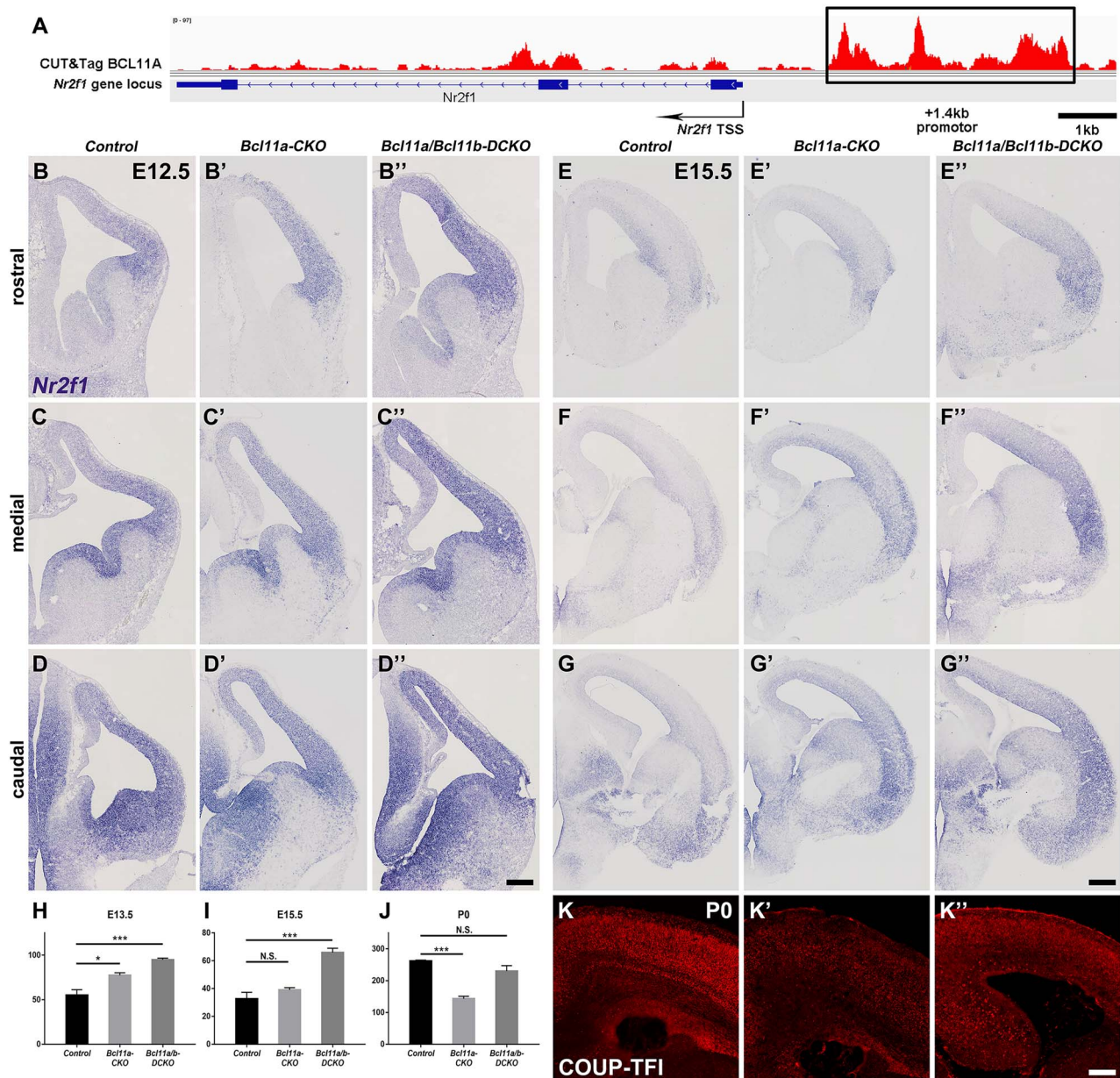


**Fig. 9.** Increased expression of *Nr2f1* in the cortices of *Bcl11a/b-DCKO* mice. (A) CUT&Tag experiments show Bcl11a binds to a conserved region of the *Nr2f1* gene. Schematic of the mouse *Nr2f1* gene locus (bottom) and CUT&Tag using a Bcl11a antibody (top) are shown. The Bcl11a binding region with a consensus binding site is shown (black rectangle). (B–D'') In situ hybridization shows *Nr2f1* expression in the control (B–D), Bcl11a-CKO (B'–D'), and Bcl11a/b-DCKO (B''–D'') mice. (E–G'') Increased *Nr2f1* expression in the ventricular zone and cortical plate of the Bcl11a-CKO (E'–G') and Bcl11a/b-DCKO (E''–G'') mice compared to the controls at E15.5 (E–G). (H–J) The FPKM value of *Nr2f1* gene based on RNA-seq data at E13.5, E15.5, and P0 (Student's t-test, N.S., not significant, \* $P < 0.05$ , \*\*\* $P < 0.001$ ,  $n = 3$ , mean  $\pm$  SEM). (K–K'') Immunohistochemistry shows *Nr2f1* expression in control (K), Bcl11a-CKO (K'), and Bcl11a/b-DCKO (K'') mice at P0. Scale bars: 200  $\mu$ m in D'' for B–D''; 300  $\mu$ m in G'' for E–G'', 200  $\mu$ m in K'' for K–K''.

## Discussion

*Bcl11a* and *Bcl11b* each play individual and essential roles in regulating cortical neurogenesis (Arlotta et al. 2005; Wiegrefe et al. 2015; Woodworth et al. 2016). However, it remains unknown whether *Bcl11a* and *Bcl11b* share joint functions and act redundantly to regulate the proliferation and differentiation of cortical progenitor cells, or the subtype specification of cortical projection neurons. Here, we show that in addition to the postmitotic

neurons, Bcl11a is expressed in cortical RGCs and intermediate progenitors, and it promotes proliferation and represses differentiation in progenitors in part through directly downregulating the expression of transcriptional factor *Nr2f1*. Our data also indicate that *Bcl11a* and *Bcl11b* function redundantly to promote the subtype specification of cortical projection neurons, especially for the deep-layer corticofugal neurons (Fig. 11). Furthermore, we find that *Bcl11a* (and possibly *Bcl11b*) prevents cortical

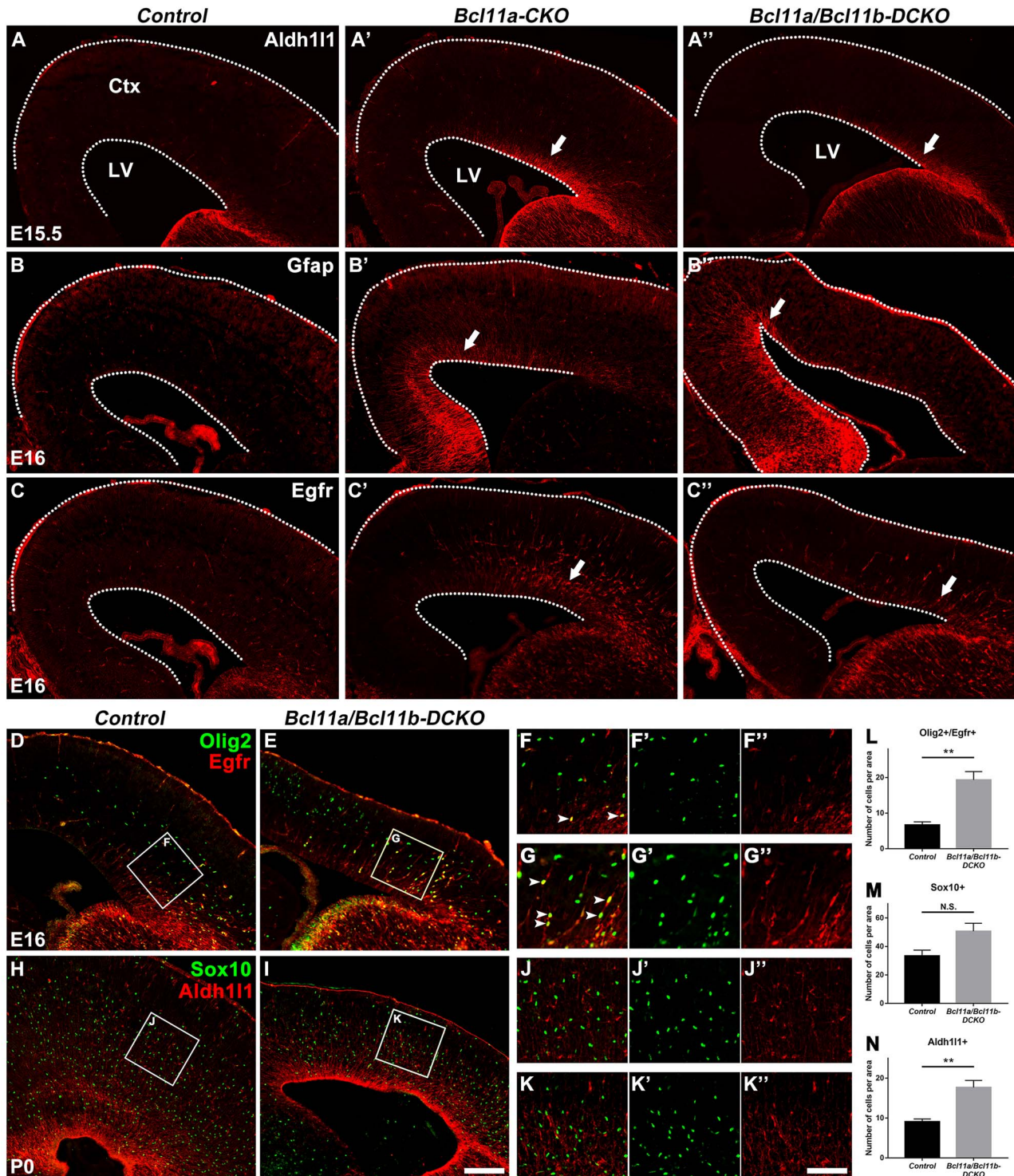


**Fig. 10.** *Bcl11a* and *Bcl11b* regulate the cortical RGC lineage progression. (A–A'') The expression of astrocytic marker *Aldh11* is markedly higher in *Bcl11a*-CKO and *Bcl11a/b*-DCKO than in control mice (arrows) at E15.5. (B–B'') The glial marker *Gfap* shows precocious expression in the cortices of *Bcl11a*-CKO and *Bcl11a/b*-DCKO mice (arrows) at E16. (C–C'') Glial progenitor marker *Egfr* shows significantly increased expression in progenitors of *Bcl11a*-CKO and *Bcl11a/b*-DCKO cortices (arrows) at E16. (D–G') *Olig2*<sup>+</sup>/*Egfr*<sup>+</sup> glial progenitors are increased in the *Bcl11a/b*-DCKO cortices compared to the control mice at E16. (H–K') *Sox10*<sup>+</sup> oligodendrocytes, *Aldh11*<sup>+</sup> astrocytes in the CP are increased in the cortices of *Bcl11a/b*-DCKO mice at P0. (L–N) Quantification of *Olig2*<sup>+</sup>/*Egfr*<sup>+</sup>, *Sox10*<sup>+</sup>, and *Aldh11*<sup>+</sup> cells at E16 or P0. (Student's *t*-test, N.S., not significant, \*\**P* < 0.01, *n* = 3, mean ± SEM) Ctx, cortex; LV, lateral ventricle. White dashed lines indicate the LV and cortex boundaries. Scale bars: 200 μm in I for A–C'', D–E, and H–I, 100 μm in K' for F–G' and J–K'.



progenitors from undergoing precocious neurogenesis to gliogenesis switch.

### **Bcl11a Regulates RGC Proliferation and Differentiation through Repressing *Coup-TFI/Nr2f1* Expression**

Previous studies reported that in the cerebral cortex, Bcl11a is only expressed in postmitotic cortical projection neurons and some cortical interneurons, and its expression is excluded from proliferating progenitors of the cortical VZ/SVZ (Wiegrefe et al. 2015). Our immunohistochemistry showed that the Bcl11a protein was detected in Pax6<sup>+</sup> cells and Eomes<sup>+</sup> intermediate progenitors at the onset of cortical neurogenesis (Fig. 1). Analysis of previously published single-cell RNA-seq data of E10.5 wild-type cortex confirmed the expression of Bcl11a in cortical progenitors (Di Bella et al. 2021). Similar expression pattern of BCL11A in the human cortex at mid-gestation week (GW17-GW18) was also observed (Supplementary Fig. S1). The expression of Bcl11a in cortical progenitors suggests that it may regulate the proliferation and differentiation of these cells. Indeed, analyses of the Bcl11a-CKO cortices revealed reduced proliferation of cortical RGCs, increased Eomes<sup>+</sup> intermediate progenitors, and precocious production of cortical projection neurons at early stages of cortical neurogenesis. Interestingly, these defects were exacerbated in the Bcl11a/b-DCKO cortices, indicating that Bcl11a and Bcl11b function jointly to regulate the proliferation and differentiation of cortical progenitor cells.

Bcl11a and Bcl11b were shown to interact with members of Coup-Tfs subfamily (Avram et al. 2000, 2002). Nr2f1 (also known as *Coup-Tf1*) is expressed in cortical progenitors and coordinately regulates cortical patterning, neurogenesis, and laminar fate (Faedo et al. 2008). Interestingly, similar to the Bcl11a-CKO and Bcl11a/b-DCKO mice, overexpression of Nr2f1 in the developing cortex led to reduced proliferation and increased neuronal differentiation (Faedo et al. 2008). We found that the expression of Nr2f1 is increased in the cortical progenitors of Bcl11a-CKO and Bcl11a/b-DCKO mice and that Bcl11a protein binds to a conserved sequence in the Nr2f1 gene. We speculate that Bcl11a promotes cortical RGC proliferation and prevents precocious neuronal differentiation through inhibiting high-level Nr2f1 expression.

### **The Redundant Functions of Bcl11 Genes in Specifying Distinct Cortical Projection Neuron Subtypes**

At E14.5, Bcl11a and Bcl11b are co-expressed in the postmitotic projection neurons in the cortical plate (Supplementary Fig. S2). When the cortical projection neurons have reached their final destination, Bcl11a is expressed in projection neurons in all cortical layers, while Bcl11b shows highest expression in the layer V subcerebral neurons and low-level expression in the layer VI neurons. Consistent with the previous report

(Woodworth et al. 2016), we observed increased Bcl11b expression in the layer VI cortical neurons in the Bcl11a-CKO mice. Further, we found that Bcl11a expression was increased in the cortical neurons of the Bcl11b-CKO mice. These results suggested the possibility that these two proteins may redundantly regulate the development of deep-layer cortical projection neurons. Previous studies have shown that in the Bcl11a-CKO mice, the numbers of layer V subcerebral neurons were increased at the expense of corticothalamic neurons and deep-layer callosal neurons (Woodworth et al. 2016) and that in the Bcl11b<sup>-/-</sup> mice, layer V subcerebral neurons, especially the corticospinal motor neurons, failed to extend axons at P0, when the mutant mice died (Arlotta et al. 2005). Our results confirmed these earlier results. In addition, we discovered that in the Bcl11a/b-DCKO mice, the deep-layer neurons showed much more severe defects in gene expression and axonal projections than the summation of the defects observed in the Bcl11a-CKO and those in the Bcl11b-CKO mice. Thus, besides the high expression of Bcl11a in corticothalamic, and deep-layer callosal neurons promotes these neurons to differentiate into their distinct subtypes and suppresses layer V subcerebral neuron identity, and Bcl11b promotes the extension and fasciculation of subcerebral axons, in particular the corticospinal tract axons in these neurons, our results indicate that these two genes might inhibit the high-level expression of each other in the differentiating neurons, and that they act redundantly to promote deep-layer neuron subtype identities.

### **Bcl11a and Bcl11b Regulate the Timing of Neurogenesis and Gliogenesis**

While Bcl11b is not expressed in proliferating progenitors during normal development, there are two possible reasons for the more severe defects in the Pax6<sup>+</sup> cells in the Bcl11a/b-DCKO cortices than the Bcl11a-CKO mice. The first possible reason is that in the absence of Bcl11a, Bcl11b expression might be upregulated in the cortical progenitors and partially compensated for the Bcl11a function in promoting progenitor cell proliferation and preventing precocious differentiation. The second possible reason is that mutant cortical projection neurons in the Bcl11a/b-DCKO mice might fail to send appropriate feedback signal to the RGCs to regulate their proliferation and differentiation. Indeed, previous studies have showed that intermediate progenitors and differentiating neurons release signaling molecules such as Delta, Jag, or Fgf9 that signal to the RGCs to regulate the cell fates of their progenies (Seuntjens et al. 2009; Parthasarathy et al. 2014; Wang et al. 2016). The Wnt7a and Wnt7b molecules that are expressed and secreted by the other radial glial cells and differentiating neurons, respectively, function in a paracrine fashion to promote the intermediate progenitors and newly generated neurons to express Delta and Jag, respectively, to activate Notch signaling in the RGCs (Wang et al. 2016). In the Bcl11a/b-DCKO cortices,

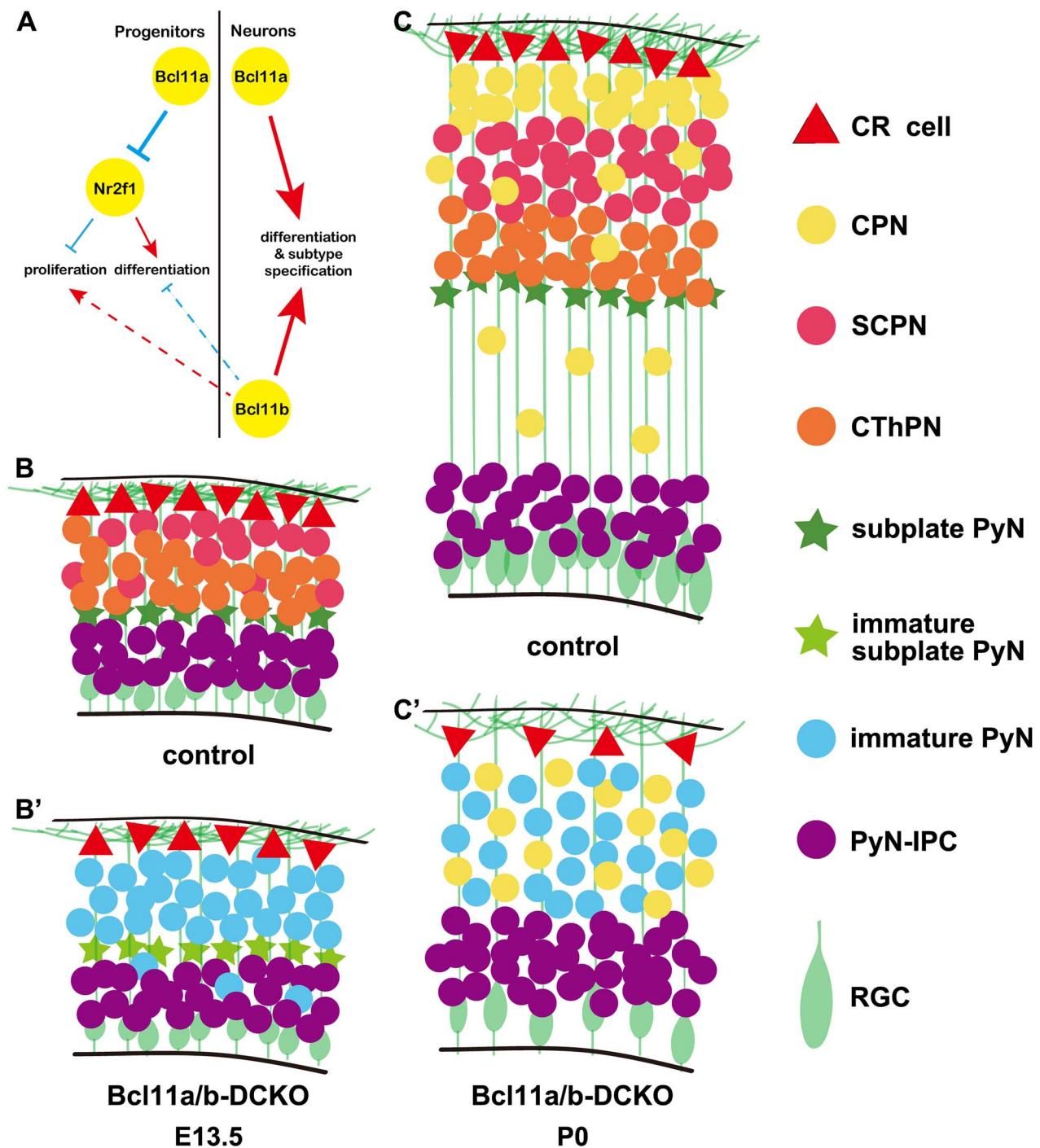


**Fig. 11.** Summary of *Bcl11a* and *Bcl11b* functions in cortical projection neuronal development. (A) An integrated diagram illustrating the genetic interactions of *Bcl11a* and *Bcl11b* play essential roles in different types of neurons. The red arrows indicate the positive regulation, while the blue arrows indicate the negative regulation. The dashed lines mean possible feedback regulations. (B–C') Conditional deletion of both *Bcl11a* and *Bcl11b* results in depletion and premature differentiation of cortical RGCs, and blockage of cortical projection neuron differentiation at E13.5 and P0. This study showed that the proper intrinsic clock of proliferation and differentiation at early neurogenesis was disrupted in the absence of *Bcl11a* and *Bcl11b*, followed by precocious RGCs lineage switch. The projection neurons of the *Bcl11a/b*-DCKO mice failed to acquire distinct subtype identities at P0. CR cell, Cajal–Retzius cells; CPN, callosal projection neurons; SCPN, subcerebral neurons; CThPN, corticothalamic neurons; PyN, projection neurons; PyN-IPC, projection neuron intermediate progenitors; RGC, radial glial cells.

the defective cortical projection neurons may fail to send the feedback signal to regulate RGC function.

At the end of cortical neurogenesis around E16.5, RGCs undergo a major lineage switch, concurrent with their gene expression change. For example, the cortical

progenitors begin to express *Aldh1l1* and *Gfap*. The cortical RGCs generate *Egfr*<sup>+</sup> intermediate progenitors instead of projection neuron intermediate progenitors. The expression of *Egfr* in the cortex is a strong indication for the onset of cortical gliogenesis (Li et al. 2021).

Surprisingly, we observed that the expression of *Aldh11l1*, *Gfap*, and *Egfr* in the *Bcl11a*-CKO and *Bcl11a/b*-DCKO cortices at an earlier stage than in the cortices of control mice (Fig. 10). This strongly suggests that cortical gliogenesis begins earlier in *Bcl11a*-CKO and *Bcl11a/b*-DCKO cortices. Thus, *Bcl11a* regulates the timing of neurogenesis-to-gliogenesis switch of cortical RGCs, and *Bcl11b* may play a joint role. However, currently we do not know how *Bcl11a* regulates this process.

### **Bcl11a/b Regulate Gene Expression through Chromatin Remodeling**

Chromatin remodeling is an important mechanism to control gene expression. It can be carried out either by covalent modification of DNA and histones or by ATP-dependent moving, ejecting, or restructuring nucleosomes (Ho and Crabtree 2010; Sokpor et al. 2018). Previous studies suggested that *Bcl11a/b* were involved in both pathways to remodel chromatin. We will focus on the possible mechanisms underlying *Bcl11a/b*-regulated gene expression during cortical development.

*Bcl11a/b* could remodel chromatin through interacting with the ATP-dependent chromatin remodeling factors such as BAF complex. *Bcl11a/b* (also known as BAF100a/b, respectively) were identified as subunits of BRG1/BRM-associated factor (BAF) complex. BAF complex, the mammalian SWI/SNF complex, hydrolyzes ATP to mobilize nucleosomes to create nucleosome-free regions of DNA (Sokpor et al. 2018). BAF complex comprises 15 subunits, which can be classified into core subunits and variant subunits. The core subunits include the BRG1 or BRM catalytic ATPase subunit and several scaffolding proteins; the variant subunits are cell type-specific and exchangeable during lineage progression (Narayanan and Tuoc 2014). In the developing central neural system, it uses Actl6a/BAF45a/d/SS18 to assemble into the neural progenitor BAF (npBAF) complex and uses Actl6b/BAF45b/c/CREST to assemble into the neuron-specific BAF (nBAF) complex (Son and Crabtree 2014). Both npBAF and nBAF complex include a *Bcl11a* or *Bcl11b* subunit. To address the possibility of *Bcl11a/b* acting as BAF subunits, we compared the cortical developmental defects resulted from BAF subunits depletion or from *Bcl11a/b* depletion. Defects in proliferation and maintenance of neural stem cells after *Bcl11a/b* depletion were similarly reported after depletion of the core ATPase subunit *Smarca4* (*Brg1*); however, reduction of cortical size seemed more severe in the *Brg1* mutants; the misregulated *Shh*-driven ventralization of dorsal cortex in the *Brg1* mutants (Zhan et al. 2011) was not observed in the *Bcl11a* and/or *Bcl11b* mutants. In addition, removing the npBAF subunit *Actla6* (BAF53a) also showed reduced cortical size, premature differentiation of cortical RGCs into IPCs, and disrupted cortical layer formation; while deletion of *Actla6* led to G2/M arrest of cortical RGCs (Braun et al. 2021), cell cycle progression seemed normal in the *Bcl11a* and/or *Bcl11b* mutants. Taken together, the similar effects of *Bcl11a/b* and BAF complex indicated

that *Bcl11a/b* possibly control cortical development as subunits of BAF complex; the distinct effects of *Bcl11a/b* and BAF complexes suggested that they may also have unique functions in cortical development.

Both of *Bcl11a/b* contain the Nucleosome Remodeling Deacetylase (NuRD) interacting domains and *Bcl11a/b* possibly function as subunits of NuRD complex to repress target gene expression. The NuRD complex couples both ATP-dependent chromatin remodeling and histone deacetylase activities. It contains multiple subunits that include the histone deacetylase proteins HDAC1/2, the chromodomain-helicase-DNA-binding protein CHD3/4, and the metastasis-associated proteins MTA1/2/3 (Hoffmann and Spengler 2019). In T lymphocytes, *Bcl11b* associated with the NuRD complex to repress targeted genes (Cismasiu et al. 2005). In neuroblastoma, *Bcl11a* recruited NuRD complexes to the promoter region of *Cdkn1c* (also names *p57KIP2*, encodes a cyclin-dependent kinase inhibitor which negatively regulates cell proliferation) and suppressed its expression (Topark-Ngarm et al. 2006). During early mouse corticogenesis, deletion of *Cdkn1c* led to increased proliferation of RGCs and IPCs followed by increased deep layer neuron production (Hoffmann and Spengler 2019). Based on our RNA-seq data, *Cdkn1c* mRNA expression was upregulated after loss of *Bcl11a/b* function (Ctr vs. DCKO, e13.5, 41.6 vs. 65.5,  $P < 0.001$ ; e15.5, 22.3 vs. 135.4,  $P < 0.001$ ). It is possible that *Bcl11a* functions together with NuRD complex to restrict *Cdkn1c* expression from RGCs, which allows the normal proliferation of RGCs. In the other words, the increased *Cdkn1c* expression resulted from *Bcl11a/b* depletion could reduce the proliferation of neural progenitors and consequently reduce the cortical size.

*Bcl11a/b* could also remodel chromatin through covalently modifying histones. *Bcl11a/b* could interact directly with the histone deacetylase Sirtuin1 (*Sirt1*) which deacetylates proteins using NAD<sup>+</sup> as a co-substrate. In vitro, *Bcl11a* recruited *Sirt1* and deacetylated chromatin-associated histones H3/H4, which led to repression of the target genes in T cells (Senawong et al. 2003, 2005). But based on scRNA-seq data, *Sirt1* mRNA was rarely expressed during cortical development. Thus, it is unlikely that *Bcl11a/b* regulated cortical development through recruiting *Sirt1*.

Taken together, *Bcl11a/b* could regulate target gene expression through ATP-dependent chromatin remodeling together with NuRD or BAF complex during cortical development.

Recent reports have revealed that *Bcl11* mutations are associated with neurodevelopmental disorders in humans. *BCL11A* has been implicated in neuropsychiatric disorders, including intellectual disability and autism spectrum disorders, while *BCL11B* was required for the formation and maintenance of synapses during development as well as in adulthood, and its deficiency has been implicated in various neurodegenerative disorders (Bae and Kim 2017; Simon et al. 2020). Our

study confirms previously reported unique functions of *Bcl11a* and *Bcl11b* in cortical neuron subtype specification and differentiation for distinct neuronal subtypes. We also show the novel function of *Bcl11a* in regulating cortical progenitor proliferation and differentiation, and the timing of neurogenesis to gliogenesis switch. In addition, we show that *Bcl11a* and *Bcl11b* function redundantly to promote the general subtype specification and differentiation of cortical projection neurons, especially for the deep-layer neuronal subtypes.

## Author Contributions

H.D. performed experiments and data analysis. Z.W., R.G., L.Y., G.L., Z.Z., Z.X., and Y.T. helped conduct experiments and analyze the data. Z.Y., X.L., and B.C. guided the project and discussed some of results. Z.Y., X.L., H.D., and B.C. designed the experiments and analyzed the results. H.D., B.C., X.L., and Z.Y. wrote the paper.

## Supplementary Material

Supplementary material can be found at *Cerebral Cortex* online.

## Notes

We are grateful to Dr. Pengtao Liu for providing the *Bcl11a<sup>Flox</sup>* and *Bcl11b<sup>Flox</sup>* mice. *Conflict of Interest*: None declared.

## Funding

National Key Research and Development Program of China (2018YFA0108000 to Z.Y.); National Natural Science Foundation of China (NSFC 31820103006 and 31630032 to Z.Y.); Shanghai Municipal Science and Technology Major Project (No. 2018SHZDZX01 to Z.Y.), ZJ Lab; Shanghai Center for Brain Science and Brain-Inspired Technology; National Natural Science Foundation of China (NSFC 32070971 to X.L.); NIH grants (R01 MH094589 and R01 NS089777 to B.C.).

## References

- Alcama EA, Chirivella L, Dautzenberg M, Dobрева G, Farinas I, Grosschedl R, McConnell SK. 2008. *Satb2* regulates callosal projection neuron identity in the developing cerebral cortex. *Neuron*. 57(3):364–377.
- Arlotta P, Molyneaux BJ, Chen J, Inoue J, Kominami R, Macklis JD. 2005. Neuronal subtype-specific genes that control corticospinal motor neuron development in vivo. *Neuron*. 45(2):207–221.
- Avram D, Fields A, Pretty On Top K, Nevriy DJ, Ishmael JE, Leid M. 2000. Isolation of a novel family of c(2)h(2) zinc finger proteins implicated in transcriptional repression mediated by chicken ovalbumin upstream promoter transcription factor (coup-tf) orphan nuclear receptors. *J Biol Chem*. 275(14):10315–10322.
- Avram D, Fields A, Senawong T, Topark-Ngarm A, Leid M. 2002. Coup-tf (chicken ovalbumin upstream promoter transcription factor)-interacting protein 1 (ctip1) is a sequence-specific DNA binding protein. *Biochem J*. 368(Pt 2):555–563.
- Bae JR, Kim SH. 2017. Synapses in neurodegenerative diseases. *BMB Rep*. 50(5):237–246.
- Balci TB, Sawyer SL, Davila J, Humphreys P, Dymont DA. 2015. Brain malformations in a patient with deletion 2p16.1: a refinement of the phenotype to *bcl11a*. *Eur J Med Genet*. 58(6–7):351–354.
- Beattie R, Postiglione MP, Burnett LE, Laukoter S, Streicher C, Pauler FM, Xiao G, Klezovitch O, Vasioukhin V, Ghashghaei TH et al. 2017. Mosaic analysis with double markers reveals distinct sequential functions of *Igl1* in neural stem cells. *Neuron*. 94(3):517–533.e513.
- Bedogni F, Hodge RD, Elsen GE, Nelson BR, Daza RA, Beyer RP, Bammler TK, Rubenstein JL, Hevner RF. 2010. *Tbr1* regulates regional and laminar identity of postmitotic neurons in developing neocortex. *Proc Natl Acad Sci U S A*. 107(29):13129–13134.
- Borello U, Madhavan M, Vilinsky I, Faedo A, Pierani A, Rubenstein J, Campbell K. 2014. *Sp8* and *coup-tf1* reciprocally regulate patterning and *fgf* signaling in cortical progenitors. *Cereb Cortex*. 24(6):1409–1421.
- Braun SMG, Petrova R, Tang J, Krokhotin A, Miller EL, Tang Y, Panagiotakos G, Crabtree GR. 2021. *Baf* subunit switching regulates chromatin accessibility to control cell cycle exit in the developing mammalian cortex. *Genes Dev*. 35(5–6):335–353.
- Britanova O, de Juan RC, Cheung A, Kwan KY, Schwark M, Gyorgy A, Vogel T, Akopov S, Mitkovski M, Agoston D et al. 2008. *Satb2* is a postmitotic determinant for upper-layer neuron specification in the neocortex. *Neuron*. 57(3):378–392.
- Canovas J, Berndt FA, Sepulveda H, Aguilar R, Veloso FA, Montecino M, Oliva C, Maass JC, Sierralta J, Kukuljan M. 2015. The specification of cortical subcortical projection neurons depends on the direct repression of *tbr1* by *ctip1/bcl11a*. *J Neurosci*. 35(19):7552–7564.
- Chan CM, Fulton J, Montiel-Duarte C, Collins HM, Bharti N, Wadelin FR, Moran PM, Mongan NP, Heery DM. 2013. A signature motif mediating selective interactions of *bcl11a* with the *nr2e/f* subfamily of orphan nuclear receptors. *Nucleic Acids Res*. 41(21):9663–9679.
- Chen B, Schaevitz LR, McConnell SK. 2005. *Fez1* regulates the differentiation and axon targeting of layer 5 subcortical projection neurons in cerebral cortex. *Proc Natl Acad Sci U S A*. 102(47):17184–17189.
- Chen B, Wang SS, Hattox AM, Rayburn H, Nelson SB, McConnell SK. 2008. The *fez2-ctip2* genetic pathway regulates the fate choice of subcortical projection neurons in the developing cerebral cortex. *Proc Natl Acad Sci U S A*. 105(32):11382–11387.
- Cismasiu VB, Adamo K, Gecewicz J, Duque J, Lin Q, Avram D. 2005. *Bcl11b* functionally associates with the NuRD complex in T lymphocytes to repress targeted promoter. *Oncogene*. 24(45):6753–6764.
- Di Bella DJ, Habibi E, Stickels RR, Scalia G, Brown J, Yadollahpour P, Yang SM, Abbate C, Biancalani T, Macosko EZ et al. 2021. Molecular logic of cellular diversification in the mouse cerebral cortex. *Nature*. 595(7868):554–559.
- Dias C, Estruch SB, Graham SA, McRae J, Sawiak SJ, Hurst JA, Joss SK, Holder SE, Morton JE, Turner C et al. 2016. *Bcl11a* haploinsufficiency causes an intellectual disability syndrome and dysregulates transcription. *Am J Hum Genet*. 99(2):253–274.
- Eckler MJ, Larkin KA, McKenna WL, Katzman S, Guo C, Roque R, Visel A, Rubenstein JL, Chen B. 2014. Multiple conserved regulatory domains promote *fez2* expression in the developing cerebral cortex. *Neural Dev*. 9:6.

- Faedo A, Tomassy GS, Ruan Y, Teichmann H, Krauss S, Pleasure SJ, Tsai SY, Tsai MJ, Studer M, Rubenstein JL. 2008. Coup-tfi coordinates cortical patterning, neurogenesis, and laminar fate and modulates mapk/erk, akt, and beta-catenin signaling. *Cereb Cortex*. 18(9):2117–2131.
- Gorski JA, Talley T, Qiu M, Puelles L, Rubenstein JL, Jones KR. 2002. Cortical excitatory neurons and glia, but not gabaergic neurons, are produced in the *emx1*-expressing lineage. *J Neurosci*. 22(15):6309–6314.
- Greig LC, Woodworth MB, Galazo MJ, Padmanabhan H, Macklis JD. 2013. Molecular logic of neocortical projection neuron specification, development and diversity. *Nat Rev Neurosci*. 14(11):755–769.
- Greig LC, Woodworth MB, Greppi C, Macklis JD. 2016. *Ctip1* controls acquisition of sensory area identity and establishment of sensory input fields in the developing neocortex. *Neuron*. 90(2):261–277.
- Guo T, Liu G, Du H, Wen Y, Wei S, Li Z, Tao G, Shang Z, Song X, Zhang Z et al. 2019. *Dlx1/2* are central and essential components in the transcriptional code for generating olfactory bulb interneurons. *Cereb Cortex*. 29(11):4831–4849.
- Han W, Kwan KY, Shim S, Lam MM, Shin Y, Xu X, Zhu Y, Li M, Sestan N. 2011. *Tbr1* directly represses *fezf2* to control the laminar origin and development of the corticospinal tract. *Proc Natl Acad Sci U S A*. 108(7):3041–3046.
- He M, Tucciarone J, Lee S, Nigro MJ, Kim Y, Levine JM, Kelly SM, Krugikov I, Wu P, Chen Y et al. 2016. Strategies and tools for combinatorial targeting of gabaergic neurons in mouse cerebral cortex. *Neuron*. 91(6):1228–1243.
- Hevner RF, Shi L, Justice N, Hsueh Y, Sheng M, Smiga S, Bulfone A, Goffinet AM, Campagnoni AT, Rubenstein JL. 2001. *Tbr1* regulates differentiation of the preplate and layer 6. *Neuron*. 29(2):353–366.
- Ho L, Crabtree GR. 2010. Chromatin remodelling during development. *Nature*. 463(7280):474–484.
- Hoffmann A, Spengler D. 2019. Chromatin remodeling complex *nurd* in neurodevelopment and neurodevelopmental disorders. *Front Genet*. 10:682.
- Juric-Sekhar G, Hevner RF. 2019. Malformations of cerebral cortex development: molecules and mechanisms. *Annu Rev Pathol*. 14:293–318.
- Kaya-Okur HS, Wu SJ, Codomo CA, Pledger ES, Bryson TD, Henikoff JG, Ahmad K, Henikoff S. 2019. Cut&tag for efficient epigenomic profiling of small samples and single cells. *Nat Commun*. 10(1):1930.
- Kwan KY, Lam MM, Krsnik Z, Kawasawa YI, Lefebvre V, Sestan N. 2008. *Sox5* postmitotically regulates migration, postmigratory differentiation, and projections of subplate and deep-layer neocortical neurons. *Proc Natl Acad Sci U S A*. 105(41):16021–16026.
- Lai T, Jabaudon D, Molyneaux BJ, Azim E, Arlotta P, Menezes JR, Macklis JD. 2008. *Sox5* controls the sequential generation of distinct corticofugal neuron subtypes. *Neuron*. 57(2):232–247.
- Leid M, Ishmael JE, Avram D, Shepherd D, Fraulob V, Dolle P. 2004. *Ctip1* and *ctip2* are differentially expressed during mouse embryogenesis. *Gene Expr Patterns*. 4(6):733–739.
- Lennon MJ, Jones SP, Lovelace MD, Guillemain GJ, Brew BJ. 2016. *Bcl11b*: a new piece to the complex puzzle of amyotrophic lateral sclerosis neuropathogenesis? *Neurotox Res*. 29(2):201–207.
- Lennon MJ, Jones SP, Lovelace MD, Guillemain GJ, Brew BJ. 2017. *Bcl11b*-a critical neurodevelopmental transcription factor-roles in health and disease. *Front Cell Neurosci*. 11:89.
- Leone DP, Srinivasan K, Chen B, Alcamo E, McConnell SK. 2008. The determination of projection neuron identity in the developing cerebral cortex. *Curr Opin Neurobiol*. 18(1):28–35.
- Lessel D, Gehbauer C, Bramswig NC, Schluth-Bolard C, Venkataramanappa S, van Gassen KLI, Hempel M, Haack TB, Baresic A, Genetti CA et al. 2018. *Bcl11b* mutations in patients affected by a neurodevelopmental disorder with reduced type 2 innate lymphoid cells. *Brain*. 141(8):2299–2311.
- Li J, Wang C, Zhang Z, Wen Y, An L, Liang Q, Xu Z, Wei S, Li W, Guo T et al. 2018. Transcription factors *sp8* and *sp9* coordinately regulate olfactory bulb interneuron development. *Cereb Cortex*. 28(9):3278–3294.
- Li P, Burke S, Wang J, Chen X, Ortiz M, Lee SC, Lu D, Campos L, Goulding D, Ng BL et al. 2010. Reprogramming of t cells to natural killer-like cells upon *bcl11b* deletion. *Science*. 329(5987):85–89.
- Li X, Liu G, Yang L, Li Z, Zhang Z, Xu Z, Cai Y, Du H, Su Z, Wang Z et al. 2021. Decoding cortical glial cell development. *Neurosci Bull*. 37(4):440–460.
- Liu N, Hargreaves VV, Zhu Q, Kurland JV, Hong J, Kim W, Sher F, Macias-Trevino C, Rogers JM, Kurita R et al. 2018. Direct promoter repression by *bcl11a* controls the fetal to adult hemoglobin switch. *Cell*. 173(2):430–442 e417.
- Liu P, Jenkins NA, Copeland NG. 2003. A highly efficient recombineering-based method for generating conditional knockout mutations. *Genome Res*. 13(3):476–484.
- Liu Z, Zhang Z, Lindtner S, Li Z, Xu Z, Wei S, Liang Q, Wen Y, Tao G, You Y et al. 2019. *Sp9* regulates medial ganglionic eminence-derived cortical interneuron development. *Cereb Cortex*. 29(6):2653–2667.
- Martynoga B, Morrison H, Price DJ, Mason JO. 2005. *Foxg1* is required for specification of ventral telencephalon and region-specific regulation of dorsal telencephalic precursor proliferation and apoptosis. *Dev Biol*. 283(1):113–127.
- McConnell SK. 1989. The determination of neuronal fate in the cerebral cortex. *Trends Neurosci*. 12(9):342–349.
- McConnell SK. 1995. Constructing the cerebral cortex: neurogenesis and fate determination. *Neuron*. 15(4):761–768.
- McKenna WL, Betancourt J, Larkin KA, Abrams B, Guo C, Rubenstein JL, Chen B. 2011. *Tbr1* and *fezf2* regulate alternate corticofugal neuronal identities during neocortical development. *J Neurosci*. 31(2):549–564.
- McKenna WL, Ortiz-Londono CF, Mathew TK, Hoang K, Katzman S, Chen B. 2015. Mutual regulation between *satb2* and *fezf2* promotes subcerebral projection neuron identity in the developing cerebral cortex. *Proc Natl Acad Sci U S A*. 112(37):11702–11707.
- Molyneaux BJ, Arlotta P, Hirata T, Hibi M, Macklis JD. 2005. *Fezl* is required for the birth and specification of corticospinal motor neurons. *Neuron*. 47(6):817–831.
- Molyneaux BJ, Arlotta P, Menezes JR, Macklis JD. 2007. Neuronal subtype specification in the cerebral cortex. *Nat Rev Neurosci*. 8(6):427–437.
- Narayanan R, Tuoc TC. 2014. Roles of chromatin remodeling *baf* complex in neural differentiation and reprogramming. *Cell Tissue Res*. 356(3):575–584.
- Parthasarathy S, Srivatsa S, Nityanandam A, Tarabykin V. 2014. *Ntf3* acts downstream of *sip1* in cortical postmitotic neurons to control progenitor cell fate through feedback signaling. *Development*. 141(17):3324–3330.
- Polioudakis D, de la Torre-Ubieta L, Langerman J, Elkins AG, Shi X, Stein JL, Vuong CK, Nichterwitz S, Gevorgian M, Opland CK et al. 2019. A single-cell transcriptomic atlas of human neocortical development during mid-gestation. *Neuron*. 103(5):785–801 e788.
- Sanders SJ, He X, Willsey AJ, Ercan-Sencicek AG, Samocha KE, Cicek AE, Murtha MT, Bal VH, Bishop SL, Dong S et al. 2015. Insights

- into autism spectrum disorder genomic architecture and biology from 71 risk loci. *Neuron*. 87(6):1215–1233.
- Senawong T, Peterson VJ, Avram D, Shepherd DM, Frye RA, Minucci S, Leid M. 2003. Involvement of the histone deacetylase sirt1 in chicken ovalbumin upstream promoter transcription factor (coup-tf)-interacting protein 2-mediated transcriptional repression. *J Biol Chem*. 278(44):43041–43050.
- Senawong T, Peterson VJ, Leid M. 2005. Bcl11a-dependent recruitment of sirt1 to a promoter template in mammalian cells results in histone deacetylation and transcriptional repression. *Arch Biochem Biophys*. 434(2):316–325.
- Seuntjens E, Nityanandam A, Miquelajauregui A, Debruyne J, Stryjewska A, Goebbels S, Nave KA, Huylebroeck D, Tarabykin V. 2009. Sip1 regulates sequential fate decisions by feedback signaling from postmitotic neurons to progenitors. *Nat Neurosci*. 12(11):1373–1380.
- Shim S, Kwan KY, Li M, Lefebvre V, Sestan N. 2012. Cis-regulatory control of corticospinal system development and evolution. *Nature*. 486(7401):74–79.
- Simon R, Brylka H, Schwegler H, Venkataramanappa S, Andratschke J, Wiegrefe C, Liu P, Fuchs E, Jenkins NA, Copeland NG et al. 2012. A dual function of bcl11b/ctip2 in hippocampal neurogenesis. *EMBO J*. 31(13):2922–2936.
- Simon R, Wiegrefe C, Britsch S. 2020. Bcl11 transcription factors regulate cortical development and function. *Front Mol Neurosci*. 13:51.
- Skene PJ, Henikoff JG, Henikoff S. 2018. Targeted in situ genome-wide profiling with high efficiency for low cell numbers. *Nat Protoc*. 13(5):1006–1019.
- Skene PJ, Henikoff S. 2017. An efficient targeted nuclease strategy for high-resolution mapping of DNA binding sites. *Elife*. 6:e21856.
- Soblet J, Dimov I, Graf von Kalckreuth C, Cano-Chervel J, Bajiot S, Pelc K, Sottiaux M, Vilain C, Smits G, Deconinck N. 2018. Bcl11a frameshift mutation associated with dyspraxia and hypotonia affecting the fine, gross, oral, and speech motor systems. *Am J Med Genet A*. 176(1):201–208.
- Sokpor G, Castro-Hernandez R, Rosenbusch J, Staiger JF, Tuoc T. 2018. Atp-dependent chromatin remodeling during cortical neurogenesis. *Front Neurosci*. 12:226.
- Son EY, Crabtree GR. 2014. The role of baf (mswi/snf) complexes in mammalian neural development. *Am J Med Genet C Semin Med Genet*. 166C(3):333–349.
- Tasic B, Yao Z, Graybuck LT, Smith KA, Nguyen TN, Bertagnolli D, Goldy J, Garren E, Economo MN, Viswanathan S et al. 2018. Shared and distinct transcriptomic cell types across neocortical areas. *Nature*. 563(7729):72–78.
- Topark-Ngarm A, Golonzhka O, Peterson VJ, Barrett B Jr, Martinez B, Crofoot K, Filtz TM, Leid M. 2006. Ctip2 associates with the NuRD complex on the promoter of p57kip2, a newly identified ctip2 target gene. *J Biol Chem*. 281(43):32272–32283.
- Trapnell C, Roberts A, Goff L, Pertea G, Kim D, Kelley DR, Pimentel H, Salzberg SL, Rinn JL, Pachter L. 2012. Differential gene and transcript expression analysis of rna-seq experiments with tophat and cufflinks. *Nat Protoc*. 7(3):562–578.
- Tsyporin J, Tastad D, Ma X, Nehme A, Finn T, Huebner L, Liu G, Gallardo D, Makhameh A, Roberts JM et al. 2021. Transcriptional repression by fezf2 restricts alternative identities of cortical projection neurons. *Cell Rep*. 35(12):109269.
- Wang W, Jossin Y, Chai G, Lien WH, Tissir F, Goffinet AM. 2016. Feedback regulation of apical progenitor fate by immature neurons through wnt7-celsr3-fzd3 signalling. *Nat Commun*. 7:10936.
- Wang Z, Zhou F, Dou Y, Tian X, Liu C, Li H, Shen H, Chen G. 2018. Melatonin alleviates intracerebral hemorrhage-induced secondary brain injury in rats via suppressing apoptosis, inflammation, oxidative stress, DNA damage, and mitochondria injury. *Transl Stroke Res*. 9(1):74–91.
- Wiegrefe C, Simon R, Peschkes K, Kling C, Strehle M, Cheng J, Srivatsa S, Liu P, Jenkins NA, Copeland NG et al. 2015. Bcl11a (ctip1) controls migration of cortical projection neurons through regulation of sema3c. *Neuron*. 87(2):311–325.
- Woodworth MB, Greig LC, Liu KX, Ippolito GC, Tucker HO, Macklis JD. 2016. Ctip1 regulates the balance between specification of distinct projection neuron subtypes in deep cortical layers. *Cell Rep*. 15(5):999–1012.
- Yoshida M, Nakashima M, Okanishi T, Kanai S, Fujimoto A, Itomi K, Morimoto M, Saito H, Kato M, Matsumoto N et al. 2018. Identification of novel bcl11a variants in patients with epileptic encephalopathy: expanding the phenotypic spectrum. *Clin Genet*. 93(2):368–373.
- Yu Y, Wang J, Khaled W, Burke S, Li P, Chen X, Yang W, Jenkins NA, Copeland NG, Zhang S et al. 2012. Bcl11a is essential for lymphoid development and negatively regulates p53. *J Exp Med*. 209(13):2467–2483.
- Zhan X, Shi X, Zhang Z, Chen Y, Wu JI. 2011. Dual role of brg chromatin remodeling factor in sonic hedgehog signaling during neural development. *Proc Natl Acad Sci U S A*. 108(31):12758–12763.
- Zhang X, Mennicke CV, Xiao G, Beattie R, Haider MA, Hippenmeyer S, Ghashghaei HT. 2020. Clonal analysis of gliogenesis in the cerebral cortex reveals stochastic expansion of glia and cell autonomous responses to egfr dosage. *Cells*. 9(12):2662.
- Zhang Y, Liu G, Guo T, Liang XG, Du H, Yang L, Bhaduri A, Li X, Xu Z, Zhang Z et al. 2020. Cortical neural stem cell lineage progression is regulated by extrinsic signaling molecule sonic hedgehog. *Cell Rep*. 30(13):4490–4504 e4494.